ELSEVIER

Palaeogeography, Palaeoclimatology, Palaeoecology 197 (2003) 171–197

PALAEO

www.elsevier.com/locate/palaeo

Depositional conditions and organic matter preservation pathways in an epicontinental environment: the Upper Jurassic Kashpir Oil Shales (Volga Basin, Russia)

A. Riboulleau [a,*], F. Baudin [b], J.-F. Deconinck [c], S. Derenne [d], C. Largeau [d], N. Tribovillard [a]

[a] *CNRS UMR PBDS, bât. SN5, Université Lille 1, 59655 Villeneuve d'Ascq cedex, France*
[b] *Département de Géologie Sédimentaire, CNRS FR32, UPMC, 4 place Jussieu, 75252 Paris cedex 05, France*
[c] *Laboratoire de Géologie, UPRES A CNRS 6143, Université de Rouen, 76821 Mont St Aignan cedex, France*
[d] *Laboratoire de Chimie Bioorganique et Organique Physique, CNRS UMR 7573, ENSCP, 11 rue Pierre et Marie Curie, 75231 Paris cedex 05, France*

Received 26 November 2001; accepted 15 April 2003

Abstract

The Middle Volgian Kashpir Oil Shales Formation, located on the Russian Platform, is a lateral equivalent of the North Sea and West Siberian petroleum source rocks. In the Volga Basin, this formation is 6 m thick and shows alternations of marls and black shales. The organic carbon content is often higher than 1%, although bioturbation and benthos are abundant, even in the black shales. In the marls, highly degraded organic matter (OM) dominates, while aliphatic, sulphur-rich OM is dominant in the black shales. The combination of sedimentological and geochemical studies allowed to determine that the redox conditions of the sediment regularly fluctuated from oxic to anoxic, under relatively productive waters, while climatic conditions were increasingly arid. It is proposed that OM deposition occurred in relation to the increasing aridity, through the combination of recurrent disruption of salinity stratification and aeolian supply of iron, which both promoted phytoplankton productivity.

Keywords: black shales; marine organic matter; geochemistry; clay minerals; climate; palaeoenvironments

1. Introduction

The Late Jurassic was a period of intense accumulation of sedimentary organic matter (OM; Hallam, 1987) and it was the second most important interval for source rock deposition, with 25% of the world hydrocarbon reserves, after the Albian–Turonian period (29% of the world reserves; Ulmishek and Klemme, 1990). Contrary to the mid-Cretaceous period, where most of OM-rich deposits can be assigned to oceanic global anoxic events (Arthur et al., 1990), the Late Jurassic was characterised by non-simultaneous OM deposition in shallow epeiric basins (Hallam,

* Tel.: +33-3-2043-4110; Fax: +33-3-2043-4910.
E-mail address: armelle.riboulleau@univ-lille1.fr (A. Riboulleau).

0031-0182/03/$ – see front matter © 2003 Elsevier B.V. All rights reserved.
doi:10.1016/S0031-0182(03)00460-7

1987; Ulmishek and Klemme, 1990; Baudin, 1995; Hantzpergue et al., 1998).

During Late Jurassic time, significant OM accumulations occurred in the northern hemisphere, especially in mid and high latitudes: on the North European Platform, with the Kimmeridge Clay Formation (sensu lato = North Sea+UK+NE France), in the Western Siberian basin, with the Bazhenov Formation and in the circum Arctic basins of North Alaska, Sverdrup basin and Barents Sea (Hallam, 1987; Ulmishek and Klemme, 1990; Leith et al., 1992). Located between these large domains, the Russian Platform was covered by a shallow epicontinental sea characterised by extensive OM deposition (Beznosov et al., 1978; Hantzpergue et al., 1998). However, in contrast to the above-mentioned basins, OM deposition was episodic and the relative stability of the platform did not allow sufficient burial of OM for hydrocarbon generation. The most important episode of OM deposition on the Russian Platform took place during the Middle Volgian, *Dorsoplanites panderi* ammonite Zone (= uppermost Lower Tithonian). Because of the short duration of deposition, the resulting OM-rich deposits are relatively thin, 8–10 m, compared to the above-mentioned formations (Russell, 1990; Vishnevskaya et al., 1999). The Middle Volgian organic-rich deposits, however, are widely distributed on the eastern and middle parts of the Russian Platform, with a total outcropping and subcropping area of more than 100 000 km^2, from the Pechora Basin in the north, to the Peri–Caspian Depression in the south, and in the Moscow Basin (Fig. 1; Markovskii, 1959; Beznosov et al., 1978; Vishnevskaya et al., 1999). Moreover, they are considered to show uniform thickness and facies distribution over the entire platform (A. Olferiev, personal communication).

In the middle Volga Basin, the OM-rich deposits from the *D. panderi* Zone are known as the Kashpir Oil Shales, from the little town where they have been mined since the 1850s (Fig. 1; Russell, 1990). As for numerous OM-enriched formations from epeiric basins (Tyson and Pearson, 1991), the Kashpir Oil Shales show decimetric to metric alternations of OM-rich and OM-lean levels. Rock Eval analyses on samples from

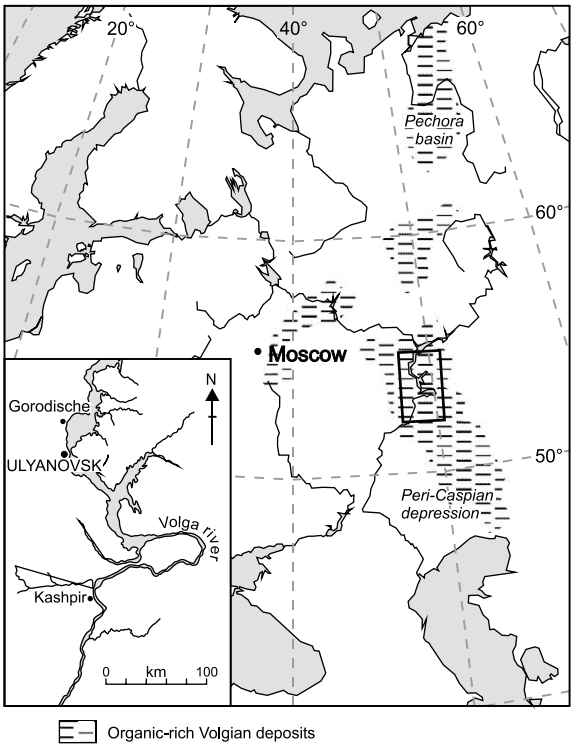

Fig. 1. Extension of the Middle Volgian organic-rich deposits of the Russian Platform (from Vishnevskaya et al., 1999) and location of the Gorodische outcrop.

different outcrops from the Volga Basin showed a high variability in OM content and quality, since organic carbon contents vary from 0.5 to 45% and the hydrogen index (HI) between 25 and 700 mg HC/g total organic carbon (TOC) (Hantzpergue et al., 1998; Riboulleau, 2000).

The aims of this study are to determine the conditions that led to the deposition of the Kashpir Oil Shales and, in particular, to understand the origin of the large quantitative and qualitative variability of OM in this deposit. The study was mainly focussed on the OM; however, the bulk sediment was also studied using calcimetry, petrography, trace metal content and clay mineralogy.

2. Geological setting and sampling

The Kashpir Oil Shales Formation was studied

on the Gorodische outcrop, located along the Volga river, 25 km north of Ulyanovsk (Fig. 1), proposed as a stratotype for the Volgian stage (Gerasimov and Mikhailov, 1966). A description of the section is given by Mesezhnikov et al. (1977). More recent sedimentological and biostratigraphical descriptions of the section, based on different taxa, were presented by Lord et al. (1987), Hantzpergue et al. (1998) and Vishnevskaya et al. (1999). The section shows ca 6 m of light to dark grey marls and calcareous clays with ammonites and belemnites that span the entire Lower Volgian (Go 5 to 8 levels of Gerasimov and Mikhailov, 1966, which could not be differentiated in the present study). The Middle Volgian deposits begin with ca 3 m of light grey marls (Go 9 and Go 10 levels), which are overlain by a 6-m-thick unit showing alternations of black shales and marls, which is the focus of this study (Go 11 level). The section ends with 2.5 m of shoreface sandstones with an erosional base, of Middle to Late Volgian age (Go 12 to 15 levels) which were not studied here.

A detailed log of the organic-rich unit (Go 11 level) is presented in Fig. 2. The formation is subdivided into 14 levels labelled *a* to *n*, from the base to the top of the unit (Fig. 2). Except for levels *f*, *g* and *i*, each level corresponds to a couplet of 5–20-cm-thick dark-coloured organic-rich mudstones termed 'black shales' and 10–70-cm-thick grey marls or calcareous clays we will refer to as 'marls'. Various shells of ammonites, bivalves, belemnites, benthic foraminifers, ostracods, as well as gasteropods, echinoid radioles and fish scales occur in both marls and black shales (Zakharov, personal communication; Rocher and Samson, unpublished report). Bioturbation and/or burrows (mainly *Planolites* and *Chondrites*) can be observed in the marls and most of the black shales (Fig. 3). The uppermost part of the unit (levels *j* to *n*) shows obvious weathering features such as oxidation of pyrite

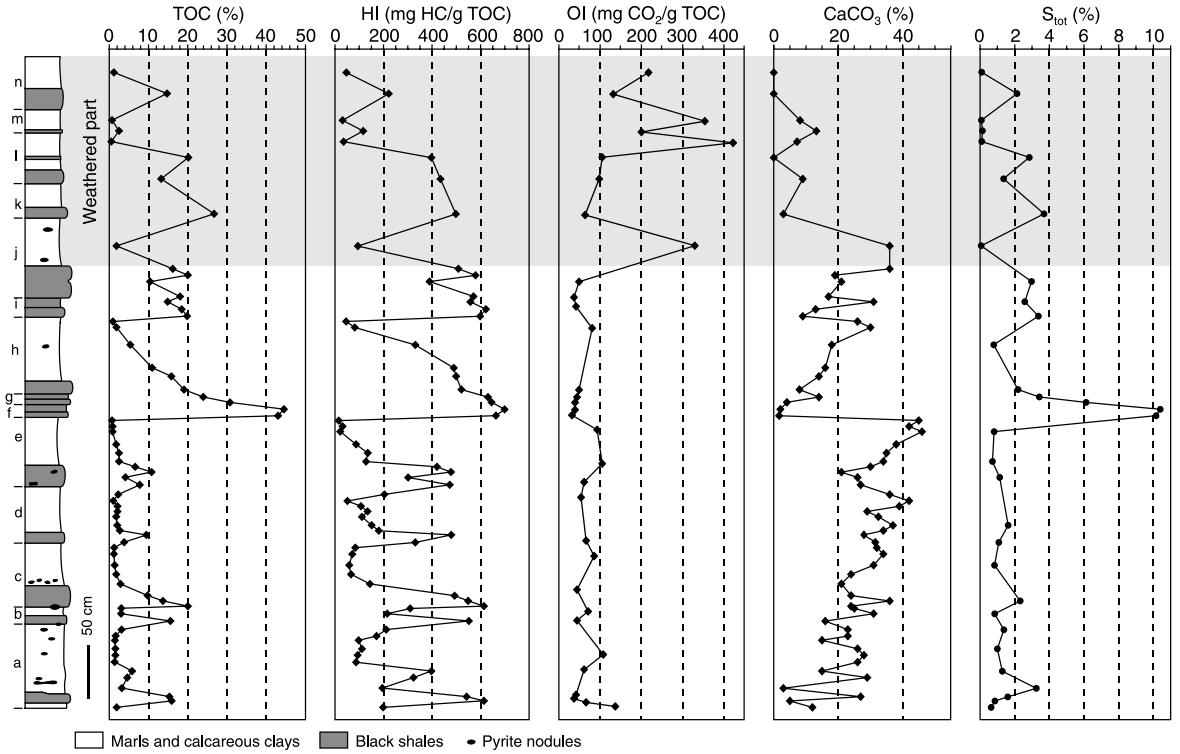

Fig. 2. Detailed log of the organic-rich unit from the Gorodische outcrop (Go 11 level) and variation of Rock–Eval parameters (TOC, HI, OI), carbonate and total sulphur content.

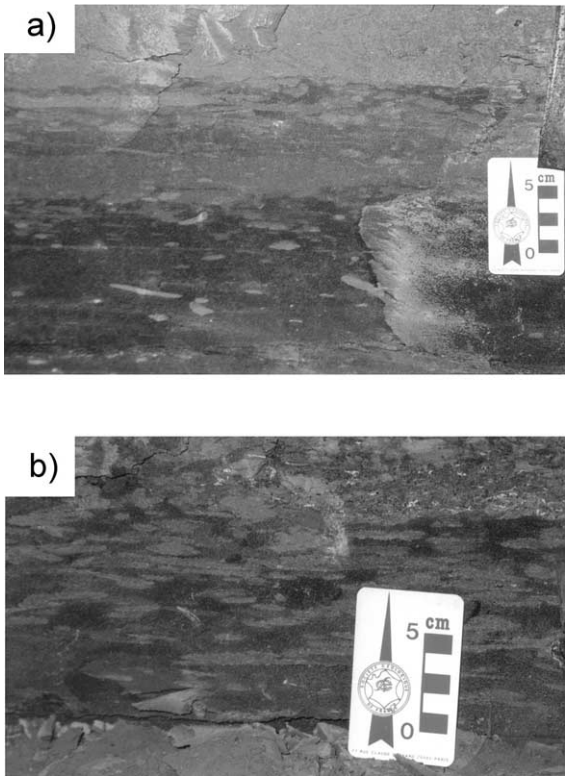

Fig. 3. Examples of bioturbations in the black shales from Gorodische section. (a) Transition from moderately burrowed black shales (bottom, TOC = 27%), to marls (top). (b) Detailed view of abundant burrows in a black shale level (TOC = 13.5%).

nodules, a lighter colour of the rocks and a fissile texture of the black shales.

A set of almost 120 samples covering the Gorodische section, among which 95 correspond to the organic-rich unit, was collected during two field trips in October 1995 and July 1999. The sampling interval varies from 5 to 50 cm beneath the organic-rich unit. A 5-10-cm interval was used for most of the organic-rich unit; a larger interval (two samples/couplet) was, however, chosen for the weathered upper part.

3. Materials and methods

Subsamples were ground for Rock Eval, LECO, trace metal content and calcimetric analyses; the remainder was stored at room temperature in darkness. Prior to further analysis, the surface of the samples was carefully removed in order to eliminate oxidised or polluted material. Rock Eval pyrolyses, OSA (Espitalié et al., 1985–1986) and Rock Eval 6 (Lafargue et al., 1998) devices, and LECO analyses were performed on 10–100-mg samples of powdered bulk rock.

Kerogens were isolated as follows: after grinding, ca 50 g of rock was extracted with $CHCl_3$/MeOH, 2:1, v/v (stirring for 12 h at room temperature) before the HCl/HF treatment (Durand and Nicaise, 1980). Palynological slides were prepared with a small part of the kerogen concentrate then obtained. The concentrate was re-extracted as described above and dried under vacuum before geochemical analyses.

The trace metal content of the bulk rock and the elemental composition of the kerogens were determined at the Service Central d'Analyses of the CNRS (Vernaison). The O content was determined by coulometry (Laboratoires Wolff, Paris). The pyrite content was determined by assuming that Fe is only present in the kerogen as pyrite.

Clay mineral associations were studied using X-ray diffraction on oriented mounts. Deflocculation of clays was done by successive washing with distilled water after decarbonatation of the crushed rock with 0.2 N HCl. The clay fraction (less than 2-μm particles) was separated by sedimentation and centrifugation (Brown and Brindley, 1980). X-ray diagrams were obtained using a Philips PW 1730 diffractometer with CuKα radiation and a Ni filter. A tube voltage of 40 kV and a tube current of 25 mA were utilised. Three X-ray diagrams were performed, after air-drying, ethylene–glycol solvation and heating at 490°C during 2 h. The goniometer scanned from 2.5 to 28.5° 2Θ for air-dried and glycol-solvated conditions and from 2.5 to 14.5° 2Θ for heating conditions. The identification of clay minerals was made according to the position of the (00l) series of basal reflections on the three X-ray diagrams (Brown and Brindley, 1980; Reynolds, 1980; Moore and Reynolds, 1989). Semiquantitative evaluations are based on the peak heights and areas summed to 100%, the relative error being about 5% (Holtzapffel, 1985; Moore and Reynolds, 1989).

4. Results

4.1. Composition of the bulk sediment

4.1.1. OM content

In Go 11 level, TOC values vary between 0.5 and 45% (Fig. 2). The unweathered part of the unit (from Go 11*a* level to the black shale of Go 11*j*) shows a high mean value of 8.7%. The HI values range from 25 to 700 mg HC/g TOC and the unweathered part shows a mean value of 312 mg HC/g TOC. The oxygen index (OI) values vary between 32 and 423 mg CO_2/g TOC. The highest OI values are observed in the uppermost weathered part of the unit (Fig. 2). T_{max} values range between 396 and 430°C. The low mean T_{max} value (416°C) indicates that the OM is immature with regards to hydrocarbon generation. Due to the small thickness of the unit, the large range in T_{max} cannot be assigned to differences in OM maturity and is rather due to differences in OM composition, as a positive trend is noted between T_{max} and OI values (Fig. 4).

On the basis of TOC and HI values, the unit comprises two distinct parts. The lower part corresponds to the Go 11*a–e* levels and shows a relatively low to medium OM enrichment, with TOC values ranging from 4 to 20% in the black shales and low TOC ($\leq 3\%$) in the marl layers. The upper part corresponds to Go 11*f–n* levels and shows a high OM enrichment, with most TOC values of black shales between 13 and 45% and marls showing TOC values up to 15%. Most of the black shales of the uppermost weathered part of the unit still show high TOC values (15–25%; Fig. 2).

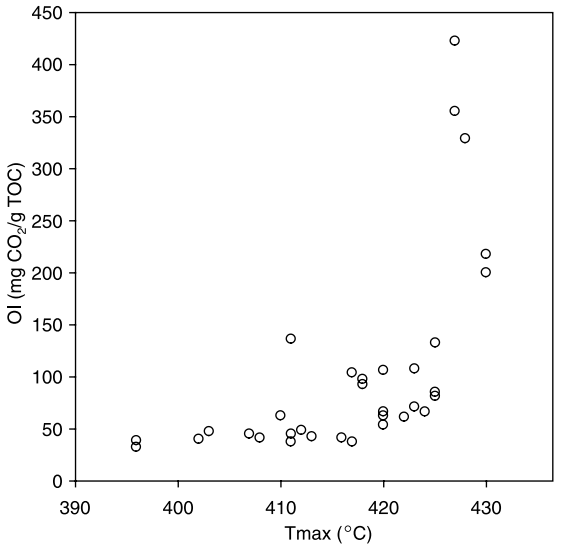

Fig. 4. Plot of the Rock–Eval parameters T_{max} and OI for the samples from Go 11 level, showing that the increase in T_{max} parameter is due to the oxidation of the OM rather than to differences in thermal maturity.

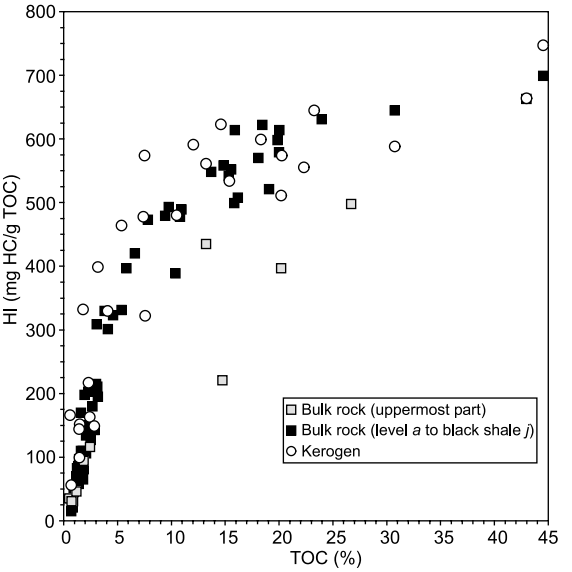

Fig. 5. Plot of the Rock–Eval parameters TOC and HI for bulk rock samples and kerogens from Go 11 level.

A positive correlation is observed between TOC and HI values of the Gorodische samples (Fig. 5). Some samples from the uppermost part of the unit (Go 11*j–n* levels), however, plot out of this correlation, despite their high TOC and/or HI values. Such a behaviour is ascribed to a decrease of HI and/or TOC of these samples caused by weathering. The general positive correlation of the unweathered samples has commonly been observed in marine recent and ancient formations (Pratt, 1984; Pradier and Bertrand, 1992; Huc et al., 1992; Lallier-Vergès et al., 1993a,b). The correlation remains similar when kerogens, instead of bulk rocks, are submitted to Rock Eval pyrolysis (Fig. 5), indicating that no mineral matrix effect influenced HI values (Espitalié et al., 1985–1986). This correlation between TOC and

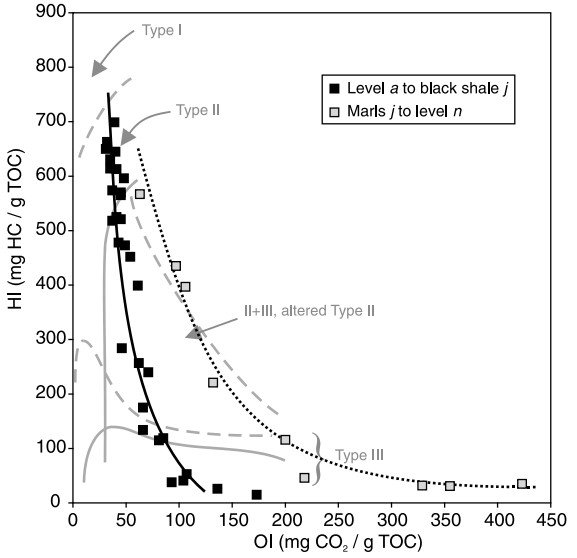

Fig. 6. Location of the samples from Go 11 level in a modified van Krevelen diagram.

HI values indicates that OM aliphaticity changes as a function of OM enrichment. This trend also reveals the mixing of one end-member which is poorly aliphatic and is dominant in OM-poor samples and another which is aliphatic and prevails in OM-rich samples. This mixing is also apparent when the samples are plotted in a modified van Krevelen diagram showing HI versus OI values where most of the samples spread along a mixing line that goes from Type II to Type III OM (Fig. 6). The samples from the uppermost part of the unit (*j–n*) are, however, characterised by higher OI values and spread along a second mixing line, roughly parallel to the first one (Fig. 6). Consistently with field observations, this different HI–OI trend once again confirms that the samples from the top of the unit are more or less weathered. The OM in these samples was, therefore, not studied in more detail.

4.1.2. $CaCO_3$ content

On the basis of the carbonate content, the two parts of the formation are clearly recognisable (Fig. 2). The lower part begins with low $CaCO_3$ contents of around 10%, which increase regularly upwards, with small fluctuations, to reach a maximum value of 46% at the top of *e* level. A sharp drop to near-zero is observed in *f* level. In the second part of the formation, the carbonate content increases again more or less regularly, from *f* to *j*. A drop in the $CaCO_3$ contents is observed in the uppermost weathered part of the formation, partly ascribed to the loss of carbonate during weathering (Littke et al., 1991). No clear trend is observed between the TOC and $CaCO_3$ contents of the unweathered samples (Fig. 7). This indicates that there is no correlation between carbonate and organic production.

4.1.3. Total sulphur content

The total sulphur content (S_{tot}) was determined for 33 samples (Fig. 2). S_{tot} values range between 0.6 and 10.4%, and their variation is clearly parallel to that of the TOC. Very low S_{tot} contents, close to 0% are observed in the weathered part of the formation, probably due to the leaching of pyrite during weathering (Littke et al., 1991), as oxidation of pyrite nodules is clearly visible in outcrop. Interestingly, the samples which show high TOC values in the weathered part of Go 11 level also show high S_{tot} contents (Fig. 2). Elemental analyses of the corresponding kerogens revealed that this sulphur is organic and not pyritic.

No gypsum was observed in the thin section; it was therefore considered that S_{tot} corresponds to

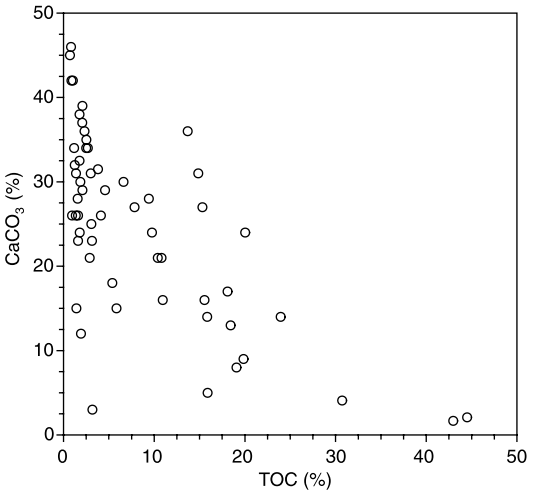

Fig. 7. Plot of the TOC versus carbonate content for the samples from the unweathered part of Go 11 level.

reduced sulphur: $S_{red} = S_{pyrite} + S_{org}$. A S_{red} versus TOC plot for the unweathered samples from Gorodische is shown in Fig. 8; a general positive correlation between the two parameters is noted, as commonly observed in recent and ancient sediments (Raiswell and Berner, 1986). One can, however, notice that the three TOC-richest samples show a different trend from the others; the samples with TOC < 25% exhibit a trend characterised by a S_{red}/TOC slope of 0.13 and a positive S_{red} axis intersect at 0.6%, while the three samples with TOC > 25% show a trend with a S_{red}/TOC slope of 0.32 and an intersect at −3.6% S_{red}. The low positive S_{red} intersect (< 2%) of the TOC < 25% samples suggests that the waters were not euxinic, which is consistent with the abundance of bioturbation and/or burrows in the sediment (cf. Leventhal, 1983). The low S_{red}/TOC slope (< 0.36) displayed by these samples would also indicate a freshwater environment (Berner and Raiswell, 1983, 1984). Normal marine conditions are, however, inferred for Gorodische from the abundance and diversity of microfossils (Lord et al., 1987). A similar low S/C slope was observed by Aller et al. (1986) in the Amazon inner shelf, despite normal salinity of bottom waters. For Amazon inner shelf, regular reoxygenation of anoxic sediments by bioturbation and

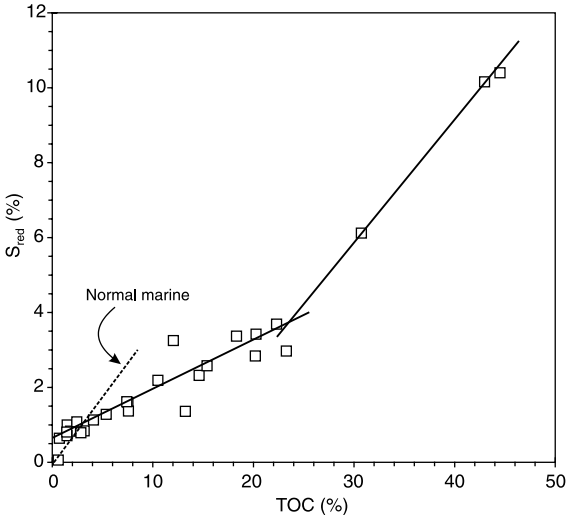

Fig. 8. Plot of the TOC versus reduced sulphur content for the samples from Go 11 level. Normal marine trend from Berner and Raiswell (1983).

remobilisation leads to reoxidation of dissolved sulphides into sulphates. Therefore, despite the high sulphate reduction rate, low levels of reduced sulphur are observed (Aller et al., 1986). Consistent with the abundance of burrows and benthic organisms in the Gorodische samples, a similar high escape of H_2S through bioturbation and/or regular reoxygenation of the upper sediment could account for the S_{red}/TOC trend of the TOC < 25% samples. The regular alternation of oxic and anoxic episodes during deposition of these samples could also account for the positive intersect of the TOC < 25% samples by the downward diffusion of sulphides in organic-poor sediments during deposition of the organic-rich levels (Passier et al., 1996). In contrast, the samples with TOC > 25% show a high S_{red}/TOC slope, close to that of normal marine sediments. These samples correspond to the entire *f* level and the base of *g*, which are the least bioturbated levels in the Gorodische section. The lack of bottom dwellers indicates that the conditions were probably anoxic during the deposition of these levels. The higher S_{red}/TOC slope observed for these samples is therefore assigned to a reduced loss/oxidation of H_2S, due to the absence of bioturbation (Berner and Westrich, 1985). From this S_{red} versus TOC plot, it therefore appears that oxygenation conditions strongly fluctuated within short time scales, during the deposition of the TOC < 25% samples while permanent anoxic conditions took place during the deposition of the OM-richest samples.

4.1.4. Trace metal content

Compared to the average trace element content of shales (Wedepohl, 1971, 1991), Go 11 level shows a high content in elements which are classically enriched in OM-rich sediments (U, V, Mo, Ni, Cu and Cr; Fig. 9). Redox-sensitive (V, Mo and U) and sulphide-forming elements (Ni and Cu) show a fairly good correlation with TOC; high trace metal contents are observed in TOC-rich levels (Fig. 10). Major exceptions to this trend are *d* level and *e* black shales which show relatively high to very high V/Al, Mo/Al, Ni/Al and Cu/Al ratios but relatively low TOC values. Detrital elements Si, Fe and, to some extent, Cr show no correlation with TOC (Fig. 10). These

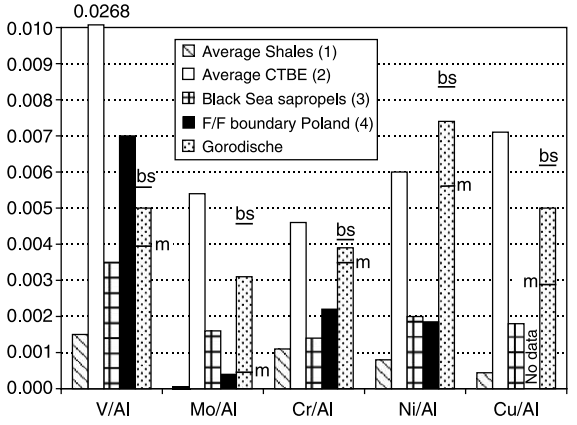

Fig. 9. Mean trace metal content normalised to Al in Go 11 level compared to average shales and different organic-rich sediments. Data from: (1) Wedepohl (1971, 1991); (2) Cenomanian–Turonian Boundary Event, Brumsack (1986) and Arthur et al. (1990); (3) Brumsack (1989); (4) Joachimski et al. (2001). m and bs: mean values for the marls and black shales, respectively.

elements show a large maximum in *d* level and *e* black shales and a second maximum in *f* and *g*. These two Si and Fe maxima also correspond to levels where both redox-sensitive and sulphide-forming elements are present in high amount.

The studied samples can be compared to other geological formations known as deposited in anoxic palaeoenvironments such as the Frasnian–Famennian boundary of Poland (Kowala section; Joachimski et al., 2001), the Cenomanian–Turonian boundary event at various locations in the Tethyan realm (Brumsack, 1986; Arthur et al., 1990), and the recent Black Sea sapropels (Brumsack, 1989). Except for V, Go 11 level shows contents in both redox-sensitive and sulphide-forming elements which are far higher than in the Black Sea sapropels and organic-rich levels from the Frasnian–Famennian boundary (Fig. 9). Higher mean trace element contents are only observed

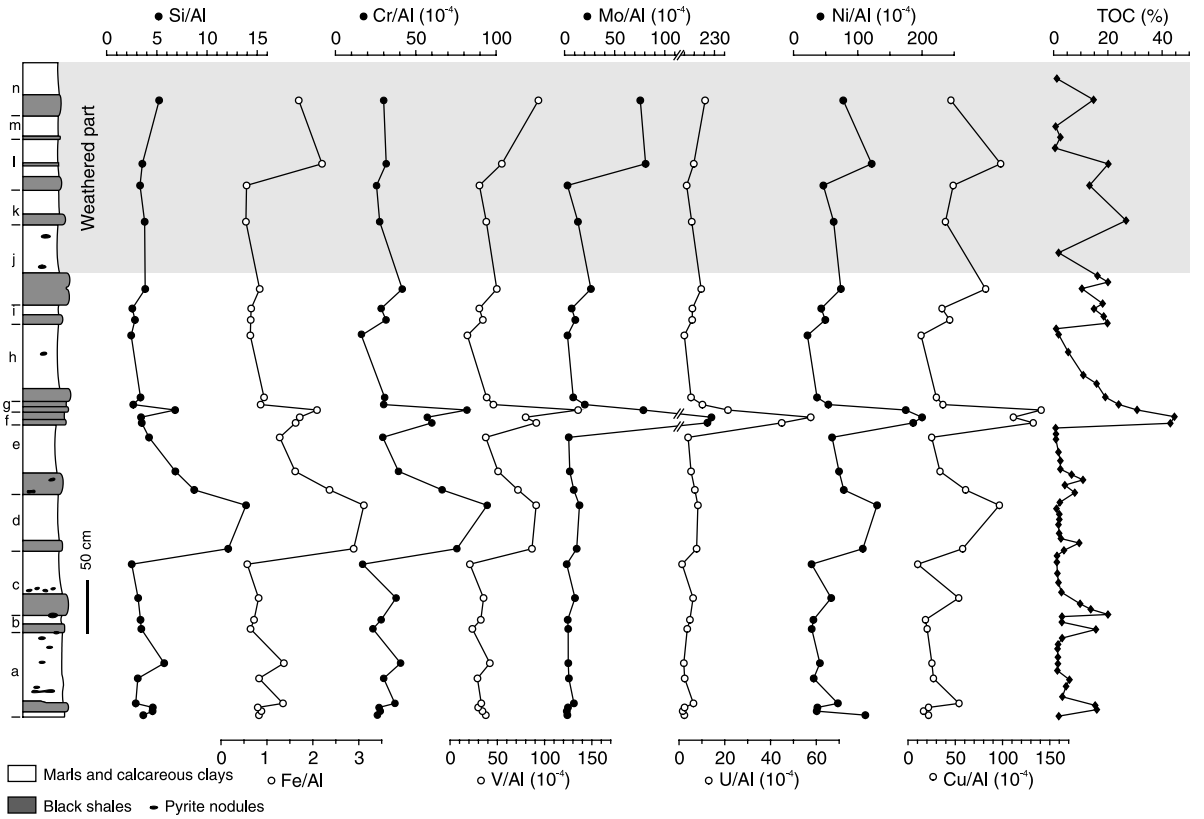

Fig. 10. Variation of the major (Si and Fe) and trace metals (Cr, V, Mo, U, Ni and Cu) normalised to Al, and organic matter content (TOC) in Go 11 level.

in samples from the CTBE (Fig. 9). The high contents in V, Mo, Cr and U in Go 11 level indicate very reducing conditions in the sediment (Brumsack, 1986; Calvert and Perdersen, 1993). Such a conclusion could seem inconsistent with the abundant burrows and benthos in the sediment. The redox front was, therefore, probably close to the sediment–water interface, leading to the anoxic character of the sediment, but episodically fell below the sediment–water interface, allowing colonisation by bottom dwellers. Such interpretation is consistent with the S_{tot}–TOC pattern which indicates strongly fluctuating oxygenation conditions during the deposition of the organic-rich unit Go 11. Ni and Cu are brought to the sediment by forming organo-metallic complexes (Brumsack, 1986; Calvert and Perdersen, 1993); their high content therefore indicates high organic inputs to the sediment, comparatively to minerals. These high organic inputs can be ascribed either to a low mineral flux and high preservation of OM under anoxic conditions or to a high primary productivity. Numerous data, such as the presence of benthic organisms, burrows, and the S_{tot}–TOC relationship indicate that the sediment–water interface was recurrently oxic, which rules out the hypothesis of OM preservation under low organic and mineral sedimentation rates. The high Ni/Al and Cu/Al are therefore considered as indicators of relatively high primary productivity.

4.1.5. Clay mineralogy

The clay mineralogy was studied in 35 samples spanning the interval from the Lower Volgian (Go 5–8 levels) to the end of *D. panderi* Zone; 22 samples correspond to the organic-rich formation. The clay minerals identified are smectite and illite–smectite mixed layers (smectites), illite, kaolinite, chlorite and palygorskite (Fig. 11). A clear trend of decreasing kaolinite and increasing smectites is observed from the base to the top of the section. This trend was previously observed by Chimkyavichus (1986) and more recently by Ruffell et al. (2002), who also examined the clay mineralogy of the Gorodische section. The studied section can be subdivided into four parts: the first part corresponds to Go 5–8 levels, where, despite small fluctuations, the clay mineralogy remains approximately constant with kaolinite ≈ 40%, illite ≈ 25%, smectites ≈ 30% and chlorite ≈ 5% (Fig. 11). The second part corresponds to Go 9 and Go 10 levels where compared to the first part, the kaolinite content is slightly decreased (≈ 30%) while smectites are increased (≈ 50%). The third part corresponds to Go 11*a* to Go 11*e* levels, where kaolinite shows a sharp decreasing trend from 30 to 10%. Conversely, smectites show a sharp increase from 50 to 70%. The fourth part, from Go 11*f* level to the top of Go 11 level, finally shows a slow decrease of kaolinite to a few per-

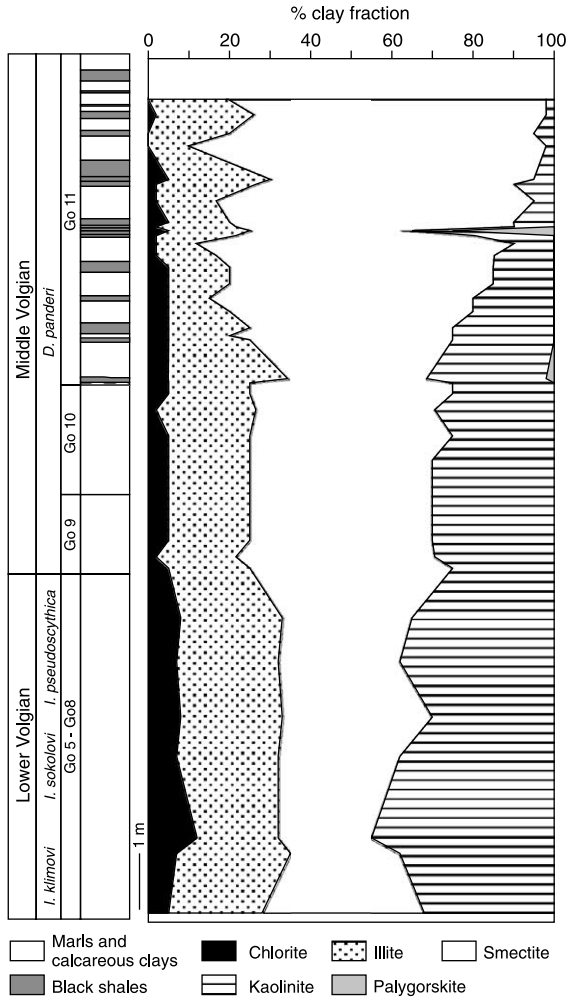

Fig. 11. Evolution of clay mineral assemblages in the Gorodische outcrop.

cent, while smectites increase up to 80% (Fig. 11). The illite content remains approximately constant through the section, while a slight decrease of chlorite is observed from the base to the top. Palygorskite was only observed in two samples: in the black shale of Go 11*a* level where it is present in low amount ($\leq 5\%$) and in the base of Go 11*g* level where it represents 25% of the clay minerals. Consistent with the results of Ruffell et al. (2002) no systematic difference is noted between the black shales and the marls in the level Go 11. Such a feature is different from other organic-rich formations where the clay mineralogy often shows a marked difference between organic-rich and organic-poor levels, e.g. Kashpir section located 150 km south of Gorodische (Fig. 1; Ruffell et al., 2002), the Kimmeridge Clay Formation (Ramdani, 1996) or the Bahloul Formation (Caron et al., 1999).

4.2. Bulk OM

4.2.1. Microfacies

The microfacies of 24 samples corresponding to marls and black shales of the unweathered part of the organic-rich unit, were observed by transmitted light microscopy in order to examine the nature and distribution of OM in the sediment. The examined samples showed very similar textures and are mainly differentiated by their content in OM particles and abundance of burrows. Most of the marls and black shales show a broadly horizontal microscopic fabric ascribed to compaction, but do not show a laminated macroscopic structure. Burrows are observed in most of the samples but with varying sizes and abundance. The mineral matrix is dominated by clays with small quartz grains whose abundance varies from 5 to 20%. Glauconite and pyrite grains are present in low amounts (a few percent). Carbonate shells (bivalves, foraminifera and ostracods) occur in most of the samples, as well as some phosphate debris. Echinoid radioles are also observed, but only in the lower part of the unit. Pyrite is present in all the samples, either as framboids, commonly associated with OM, or as replacement of carbonate shells.

Three classes of OM are distinguished: small black woody debris, diffuse OM and yellow to red lenses. The black woody debris, corresponding to terrestrially derived particles, are rare in all the samples. The diffuse OM appears as a dark brown colouration of the mineral matrix rather than well-shaped particles (Fig. 12a), and probably corresponds to the organo-mineral groundmass as described by Bertrand et al. (1990) for samples from the Kimmeridge Clay Formation. Such OM is commonly observed in the burrows and proved difficult to quantify. The diffuse OM is generally the major form of OM observed in the marl layers. The yellow to red lenses usually present elongated shapes, with a length ranging from a few tens of μm to 1 mm. These lenses are distributed in the sediment (Fig. 12c) but also occur as bundles. Their abundance in the samples is highly variable, but clearly parallels TOC variations: almost absent from low-TOC samples, they constitute most of the sediment in the TOC-richest samples (Fig. 12e).

4.2.2. Palynological observations

Palynological observations of the total residue after acid digestion of the mineral matrix were performed by transmitted light microscopy on 24 samples from the unweathered part of the organic-rich unit. All the examined samples are dominated by amorphous OM (AOM), which generally represents more than 90% of the palynofacies. Palynomorphs are dominated by small black woody debris (PM4, according to the classification of Whitaker, 1984). Algal remains are also relatively abundant among the palynomorphs and dominated by dinocysts; rare tasmanaceans are also present in a few samples.

Based on their colour and texture, three classes of amorphous particles can be distinguished in palynofacies: dark grey to brown fluffy particles, commonly associated with small pyrite crystals (grey AOM; Fig. 12b), yellow to orange heterogeneous aggregates (heterogeneous orange AOM; Fig. 12d) and orange homogeneous gel-like particles (pure orange AOM; Fig. 12f), similar to those previously observed in S-rich samples from the Kimmeridge Clay Formation (Boussafir et al., 1995) and the Orbagnoux lagoonal deposits (Mongenot et al., 1999). On the basis of morpho-

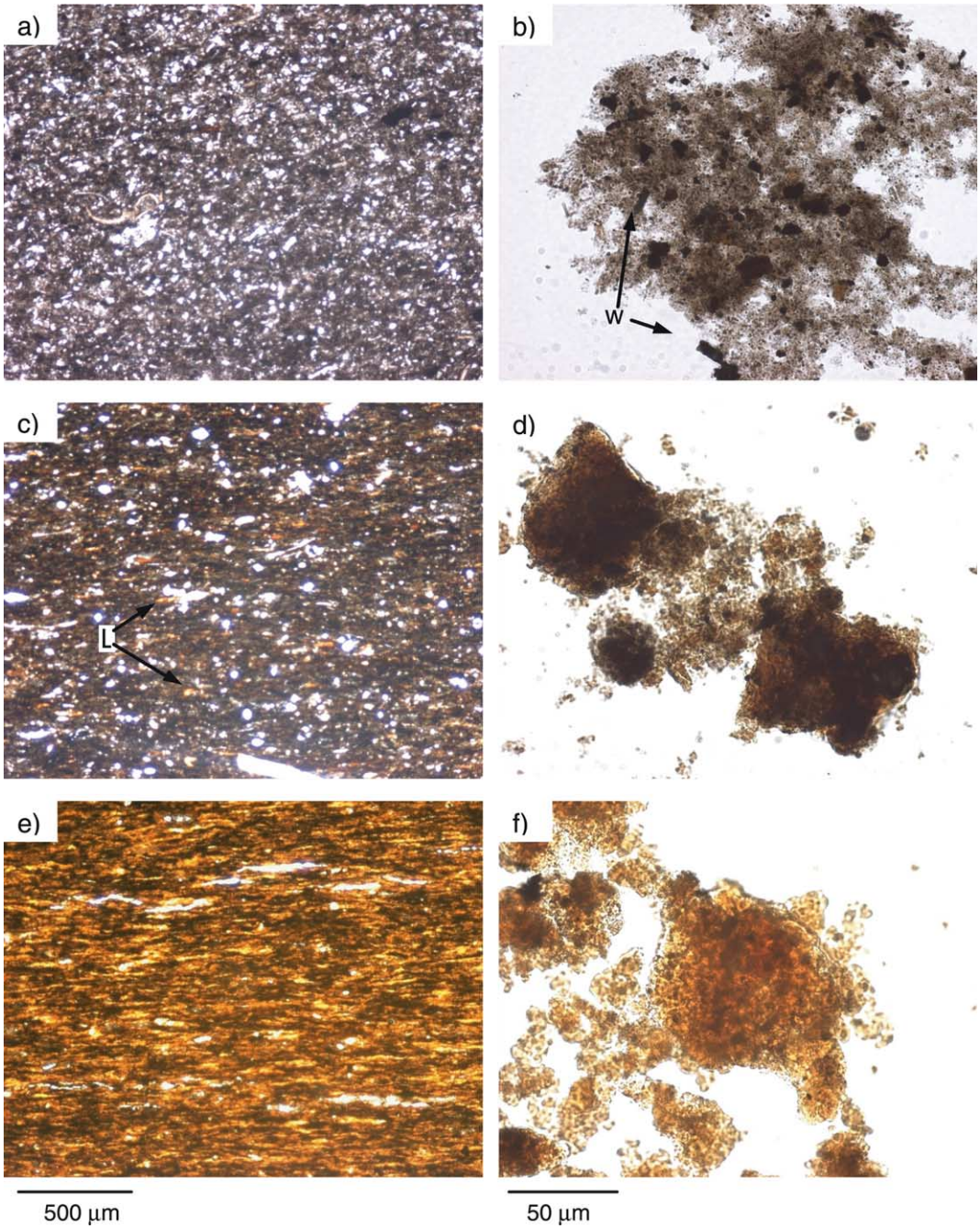

Fig. 12. Thin sections (a,c,e) and palynological (b,d,f) microphotographs of three typical samples. (a) Marly layer Go 11 *aBS base*. The sample is mainly composed of clays and quartz. No organic orange lens is visible, the grey colour of the matrix is partly due to diffuse OM. (b) Kerogen from the same sample. Grey amorphous organic particles, associated with small woody debris (w) and small pyrite framboids. (c) Black shale layer Go 11 *aBS top*. The sample is mainly composed of clays; quartz grains are less abundant than in the previous sample. Orange to yellow organic lenses (L) are widespread in the sample. (d) Kerogen from the same sample. Heterogeneous orange amorphous organic particles dominate the palynofacies. (e) Black shale Go 11 *f top*. The sample is largely dominated by orange to yellow organic lenses; rare quartz grains are observed. (f) Kerogen from the same sample. Pure orange amorphous organic particles dominate the palynofacies.

logical characteristics, heterogeneous orange particles seemed intermediate between the two other classes. Counting of particles showed that only one of these classes is dominant per sample. In addition, a good correlation is noted between the dominant class of AOM and the bulk parameters of the samples (Fig. 13). Samples with low TOC and HI are dominated by grey AOM whereas samples with the highest TOC and HI are dominated by pure orange AOM; the samples with intermediate values are dominated by the heterogeneous orange AOM (Fig. 13), which corroborates the intermediate nature of these particles. Similar correlations between TOC and proportion of different palynological and petrographical classes of OM were previously observed in the Kimmeridge Clay Formation (Pradier and Bertrand, 1992; Ramanampisoa et al., 1992; Boussafir, 1994) and in its lateral equivalent in France (Bialkowski et al., 2000; Tribovillard et al., 2001). In particular, the increasing contribution of orange gel-like AOM was parallel to the increase in TOC (Ramanampisoa et al., 1992; Boussafir, 1994; Bialkowski et al., 2000).

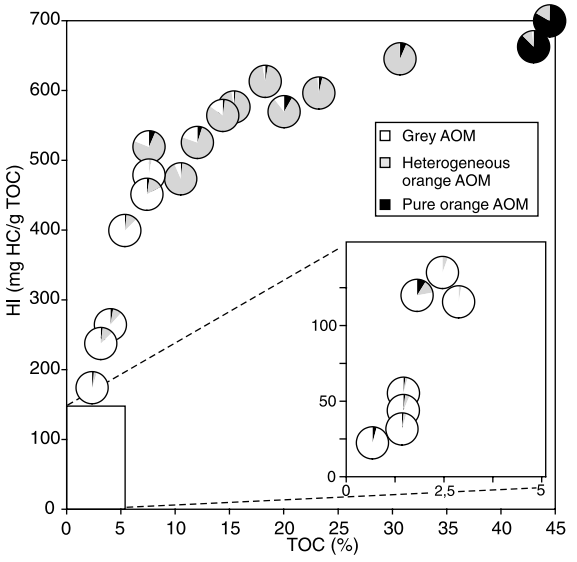

Fig. 13. Plot showing the positive correlation between TOC, HI and the composition of the palynofacies (circular diagrams) of the samples from the organic-rich formation from Gorodische outcrop.

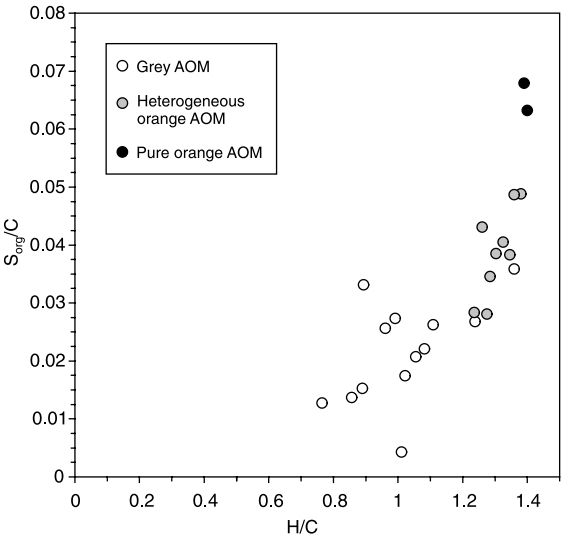

Fig. 14. Variation of the atomic ratios H/C versus S_{org}/C of the kerogens from Go 11 level.

4.2.3. Elemental analysis

H/C and S_{org}/C ratios of the kerogens were determined from the elemental analysis data, by assuming that Fe is only present in the residues as pyrite. The atomic H/C ratios vary between 0.76 and 1.40 and are well correlated with HI values of the bulk rock. The atomic S_{org}/C ratios vary between 0.004 and 0.068. Six samples are characterised by $S_{org}/C \geq 0.040$, indicating that they correspond to Type II-S OM as defined by Orr (1986). A positive trend is observed between H/C and S_{org}/C ratios (Fig. 14); such a correlation between aliphaticity and sulphur content of kerogens has been previously observed in the Kimmeridge Clay Formation (Lallier-Vergès et al., 1993b) and indicates that natural sulphurisation mostly involved aliphatic units such as lipids and carbohydrates.

In addition to their morphological features, the different classes of AOM are characterised by contrasting elemental compositions: the pure orange AOM is highly aliphatic (H/C ca 1.4) and S-rich ($S_{org}/C > 0.060$), while the grey AOM is poorly aliphatic (mean H/C ca 1) and relatively S-poor (mean $S_{org}/C = 0.022$; Fig. 14). The heterogeneous orange AOM is aliphatic (mean H/C = 1.3) but moderately enriched in S_{org} (mean $S_{org}/C = 0.039$; Fig. 14). These elemental analyses confirm the intermediate character of the heteroge-

neous orange particles; moreover, it appears that the AOM classes identified by light microscopy also correspond to chemical classes. These observations are relatively similar to those of Boussafir et al. (1995) in the Kimmeridge Clay Formation and corroborate the observations of Boussafir et al. (1995) and Mongenot et al. (1999), indicating that natural sulphurisation is the main pathway responsible for the formation of gel-like orange AOM.

4.2.4. Sulphur speciation

The pyritic- and organic-sulphur contents of the crude rock samples (S^*_{pyr} and S^*_{org}) were determined on the basis of total sulphur content and S and Fe elemental analysis of the kerogen concentrates. Whatever the TOC value of the sediment, S^*_{pyr} remains approximately constant around 0.75% (Fig. 15). By contrast, S^*_{org} increases regularly with TOC (Fig. 15). Such a behaviour of sulphur species is frequently observed in carbonate environments (see, for example, Bein et al., 1990) and indicates that pyrite formation is Fe limited. In the present case, the mean $CaCO_3$ content being lower than 25%, the sedimentation was dominated by detrital minerals, which are generally accompanied by reactive Fe species. This is confirmed by the high mean Fe/Al ratio of Gorodische samples when compared to average shales (1.25 vs 0.54; Wedepohl, 1971, 1991). It therefore appears that inputs of detrital iron were not low. As Gorodische setting was located far away from clastic inputs (Thierry et al., 2000), specific loss of reactive Fe species during transport may have occurred (Suits and Arthur, 2000). However, it is more likely that iron limitation occurred due to very high production of reduced sulphur in the sediment, induced by very high inputs of metabolisable OM and high sulphate reduction rates. A similar iron limitation in a clayey environment was previously observed in the case of the very organic-rich cycles from the Kimmeridge Clay Formation (Lallier-Vergès et al., 1993b, 1995; Tribovillard et al., 1994).

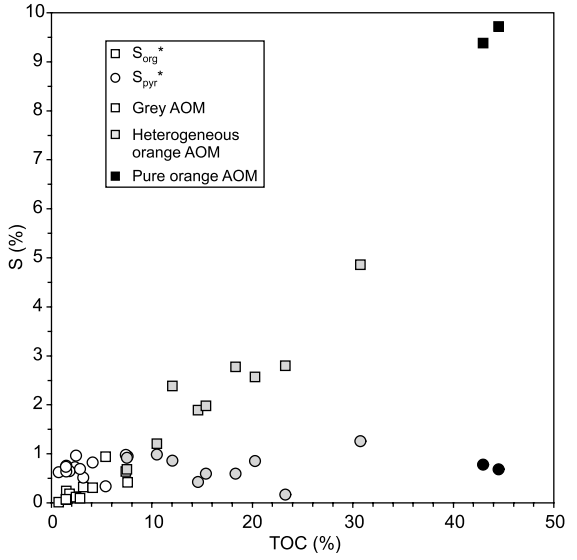

Fig. 15. Variation of the pyritic- (S^*_{pyr}) and organic-sulphur (S^*_{org}) content as a function of TOC for the bulk samples from Go 11 level.

4.3. Detailed study of selected kerogens

Study of the bulk OM showed that in the Gorodische section, the observed quantitative and qualitative variations are due to the different contributions of two types of OM: one which is very aliphatic and dominates in the OM-richest samples (pure orange AOM) and one which is less aliphatic and dominates in the OM-poorest samples (grey AOM). Intermediate samples are dominated by the heterogeneous orange AOM which should correspond to mixing of the two above types of OM particles.

In order to check this hypothesis, to go further in the characterisation of OM sources and preservation pathway(s), and to propose a reconstruction of the depositional conditions, three kerogens, each one dominated by a different class of AOM, were studied using microscopic and pyrolytic techniques. The three selected samples are: *aBS base*, from the very base of Go 11*a* level, for grey AOM, *aBS top*, from the black shales of Go 11*a* level, for heterogeneous orange AOM, and *f top*, from Go 11*f* level, for pure orange AOM (Table 1). *ABS base* kerogen is poorly aliphatic and S_{org} lean, while *f top* kerogen is both aliphatic and enriched in S_{org} (Type II-S kerogen). *ABS top* kerogen is aliphatic and moderately enriched in S_{org}. The detailed microscopic and geochemical

Table 1
Bulk rock and kerogen characteristics of the three selected samples

	Bulk rock			Kerogen[a]		
Sample	TOC (%)	HI[b]	OI[c]	H/C	O/C	S_{org}/C
aBS base	2.3	175	66	0.96	0.27	0.026
aBS top	12.0	525	41	1.35	0.18	0.038
f top	44.5	699	39	1.39	0.20	0.068

[a] Atomic ratios.
[b] mg HC/g TOC.
[c] mg CO_2/g TOC.

studies of these three kerogens were reported elsewhere (Riboulleau, 2000; Riboulleau et al., 2000, 2001) and only major results are briefly summarised here.

When examined by transmission electron microscopy (TEM), the three kerogens appeared to mainly comprise a structureless organic matrix (nanoscopically AOM). However, some thick cell walls (ca 200 nm thick), probably corresponding to dinocysts, and thin cell walls (10–50 nm thick) associated into bundles termed *ultralaminae* (Largeau et al., 1990) were observed. *Ultralaminae* are present in low amount in *aBS base*, and in minor amount in *aBS top*. Cell walls, and particularly *ultralaminae*, have been previously detected by TEM observations of numerous kerogens and correspond to the cell walls of microscopic algae preserved by the so-called 'selective preservation' pathway (Raynaud et al., 1989; Largeau et al., 1990; Derenne et al., 1991). The low abundance of recognisable cell walls and *ultralaminae* in *aBS base* and *aBS top* and their absence in *f top* indicate that the selective preservation pathway only played a minor role in the formation of these kerogens and, therefore, that other preservation processes were involved.

The different OM preservation pathways currently recognised are selective preservation, degradation–recondensation, and natural sulphurisation, also termed vulcanisation. While selective preservation can be readily characterised by TEM observations, different methods are necessary for the characterisation of the other preservation pathways, since they lead to the formation of nanoscopically AOM (Boussafir et al., 1995; Zegouagh et al., 1999). Pyrolytic techniques proved powerful in characterising the natural sulphurisation and degradation–recondensation pathways; the former is characterised by abundant production of sulphur-containing products (Sinninghe Damsté and de Leeuw, 1989) and the latter is characterised by low pyrolysis yields and production of aromatic compounds (Zegouagh et al., 1999; Poirier et al., 2000). A complete pyrolytic study was therefore performed on the three kerogens (Riboulleau, 2000; Riboulleau et al., 2000, 2001). The pyrolysis products obtained for the three kerogens were dominated by $C_{\leq 24}$ linear compounds, revealing a dominant contribution of phytoplanktonic material. A small contribution of bacterial lipids was also noticed from the presence of branched compounds and hopanoids. The contribution of terrestrial material appeared minor for the three kerogens, as indicated by the absence of long-chain alkanes and lignin-derived phenols, which is in agreement with palynological observations.

The contribution of the different preservation pathways, deduced from the detailed study of the three kerogens, is summarised in Table 2. The abundance of S-containing compounds, and particularly of short-chain ones, in *f top* pyrolysate indicated formation of this kerogen by sulphurisation of planktonic lipids and carbohydrates (Riboulleau et al., 2000). *ABS base* kerogen, on the basis of its low aliphaticity, high oxygen content and low yields upon pyroly-

Table 2
OM preservation processes of the three selected samples as deduced from the detailed study of the kerogen

Preservation pathway	Resulting material	*aBS base*	*aBS top*	*f top*
Selective preservation	Algal cell walls	+	+/−	−
Natural sulphurisation	Sulphurised OM	−	++	++ ++
Degradation–recondensation	Melanoidins	+++	+	−

−: minor to non-existent.

sis was shown to be mainly constituted of melanoidin-like macromolecules, formed by the degradation–recondensation pathway in addition to the low contribution of selectively preserved material observed by TEM (Riboulleau et al., 2001). *ABS top* kerogen appeared to be constituted of both melanoidin units and sulphurised lipids and carbohydrates (Riboulleau, 2000).

5. Depositional conditions of the different classes of AOM

The geochemical study of bulk rock samples and elemental analysis of kerogens indicated that the AOM classes determined by light microscopy also correspond to chemical classes. Since these classes are relatively homogeneous, the results obtained by the detailed study of the selected kerogens can be extended to all the samples from the same class. The different OM preservation processes indicated by the detailed study of the three selected kerogens require contrasting early diagenetic conditions (Table 2). In the light of the bulk geochemical data and OM preservation pathways, the depositional conditions of each class of AOM can therefore be determined.

5.1. Grey AOM

The detailed geochemical study of *aBS base* kerogen revealed that the grey AOM mainly corresponds to poorly aliphatic melanoidin-like material formed by the so-called 'degradation–recondensation' pathway and to a lesser extent also contains selectively preserved resistant algal cell walls (Table 2; Riboulleau et al., 2001).

In the marine environment, melanoidin-like compounds are formed from random polymerisation of degradation products of carbohydrates and proteins (Tissot and Welte, 1978). Such components attest for relatively intense biodegradation and rather indicate well-oxygenated conditions for the samples dominated by the grey AOM. For example, the predominance of melanoidin-like compounds has been previously observed in different oxic environments such as soils (van Bergen et al., 1997; Poirier et al., 2000), marine water columns (van Heemst et al., 1993; Peulvé et al., 1996) and oxygenated sediments from the Northwest African upwelling area (Zegouagh et al., 1999).

Grey AOM is dominant in the samples with the lowest TOC contents and HI values, which mainly correspond to the marl layers. Most of the marl layers from the Gorodische section show a diverse and abundant benthic fauna (Lord et al., 1987; V. Zakharov, personal communication) and are thoroughly bioturbated, indicating generally good oxygenation conditions of bottom waters and upper sediment. The OM preservation pathways determined for *aBS base* kerogen, and for grey AOM-dominated samples, are therefore consistent with sedimentological data. The high amount of redox-sensitive trace elements in the marl layers compared to average shales, however, testifies for recurrent episodes of dysoxia to anoxia during deposition of these levels (Fig. 9). These contrasting data are not inconsistent if we consider either that the oxic front was close to the sediment–water interface, but not enough to hinder benthos development, or that relatively short-term fluctuations of the oxic front occurred, allowing deposition of OM and fixation of redox-sensitive trace elements during low-oxygenation periods and colonisation by benthos, bioturbation of the sediment and degradation of the OM during more-oxygenated periods. Such a scenario is consistent with the fact that the proportion of grey AOM in the sediment (i.e. % grey AOM × TOC) in Go 11 level shows no correlation with redox-sensitive and sulphide-forming elements (Fig. 16a,b). As previously discussed, the high Ni/Al and Cu/Al ratios of the marls compared to other organic-rich deposits are interpreted as indicating a relatively high primary productivity (Fig. 9). It therefore appears that despite high OM inputs and recurrent anoxia to dysoxia, the low TOC and HI of the grey AOM-dominated samples are due to regular oxygenation of the upper sediment (Fig. 17a).

5.2. Pure orange AOM

The pure orange AOM is dominant in the two OM-richest samples from Gorodische, showing

TOC values >40% and both located in the Go 11*f* level. As previously noted, and by contrast with the other samples from the section, the absence of burrows and benthos indicates that this level was deposited under permanently anoxic conditions. This is confirmed by the very high V/Al, Mo/Al and U/Al ratios in these samples (Fig. 10). The detailed geochemical study of *f top* revealed that the pure orange AOM was predominantly preserved by natural sulphurisation (Table 2; Riboulleau et al., 2000). Natural sulphurisation of OM requires specific early diagenetic conditions including anoxia of the sediment, presence of metabolisable OM, abundant release of HS^-/H_2S by sulphate reduction and low contents of reactive Fe so that reduced sulphur can react with the reactive OM (Sinninghe Damsté and de Leeuw, 1989).

The very high TOC content of *f* level implies that OM represents more than 70% volume of the whole sediment and, consequently, that minerals only represent less than 30%. It is highly improbable that such a high amount of OM could accumulate as the result of a single decrease of the diluting mineral flux, without any increase of the primary productivity. Even under an anoxic water column, the decrease of the mineral flux – either detrital or biogenic – implies higher exposure of the OM to biodegradation. Hulthe et al. (1998) recently demonstrated that under anoxic conditions, very labile OM such as proteins and carbohydrates would be as efficiently biodegraded as in aerobic conditions. As carbohydrates and proteins remains are present in *f top* kerogen (Riboulleau et al., 2000; Mongenot et al., 2001), it is inferred that these molecules could escape remineralisation due to rapid accumulation of the OM. A very high rate of organic sedimentation due to a very high phytoplanktonic productivity is therefore more likely, which is consistent with the very low proportion of woody debris to AOM in the palynofacies, and the very high Ni/Al and Cu/Al ratios of *f* level (Fig. 10). These eutrophic conditions were associated with a high oxygen consumption leading to a rise of the anoxic front above the sediment–water interface, which is consistent with the absence of bioturbation and benthic fauna in this level (Fig. 17c). The very high primary productivity also led to a high exportation of metabolisable OM to the sediment and to a high rate of sulphate reduction. The presence of both high H_2S production, high amounts of reactive OM and insufficient amounts of reactive Fe in the sediment led to massive OM sulphurisation. The presence of ammonite shells and belemnite rostra in the sediment, however, indicates that the upper water layer was relatively well oxygenated (Fig. 17c). This is consistent with the absence of biomarkers of green sulphur bacteria, indicators of photic zone anoxia, in the pyrolysis products of *f top* kerogen (Riboulleau et al., 2000).

5.3. Heterogeneous orange AOM

As shown by bulk studies of the Gorodische samples and a detailed study of *aBS top* kerogen, the heterogeneous orange particles correspond to a mixture of the two other classes of particles (Table 2). The presence of melanoidin-like material and selectively preserved algal cell walls in the kerogens points to a relatively high level of biodegradation of the OM, while the presence of sulphurised material would rather indicate the relative persistence of eutrophic conditions as described for the pure orange AOM. The combination of these contrasting OM preservation pathways is once again consistent with the conclusion that strongly fluctuating oxygenation conditions, from oxic to anoxic, occurred during the deposition of the organic-rich unit Go 11.

Most of the samples dominated by heterogeneous orange AOM correspond to black shales. From the higher mean contents of V, Mo, U, Ni and Cu in the black shales than in the marls (Fig. 9), more severe dysoxia and higher primary productivity are inferred during deposition of these levels (Fig. 17b). Due to the general covariation of redox-sensitive and sulphide-forming trace elements (Fig. 10), it seems highly probable that dysoxia is, at least partly, productivity induced. In any case, for the samples with (% pure+% heterogeneous orange AOM)×TOC > 5%, the proportion of total orange AOM to the sediment shows a positive trend with both redox-sensitive and sulphide-forming elements (Fig. 16c,d). This

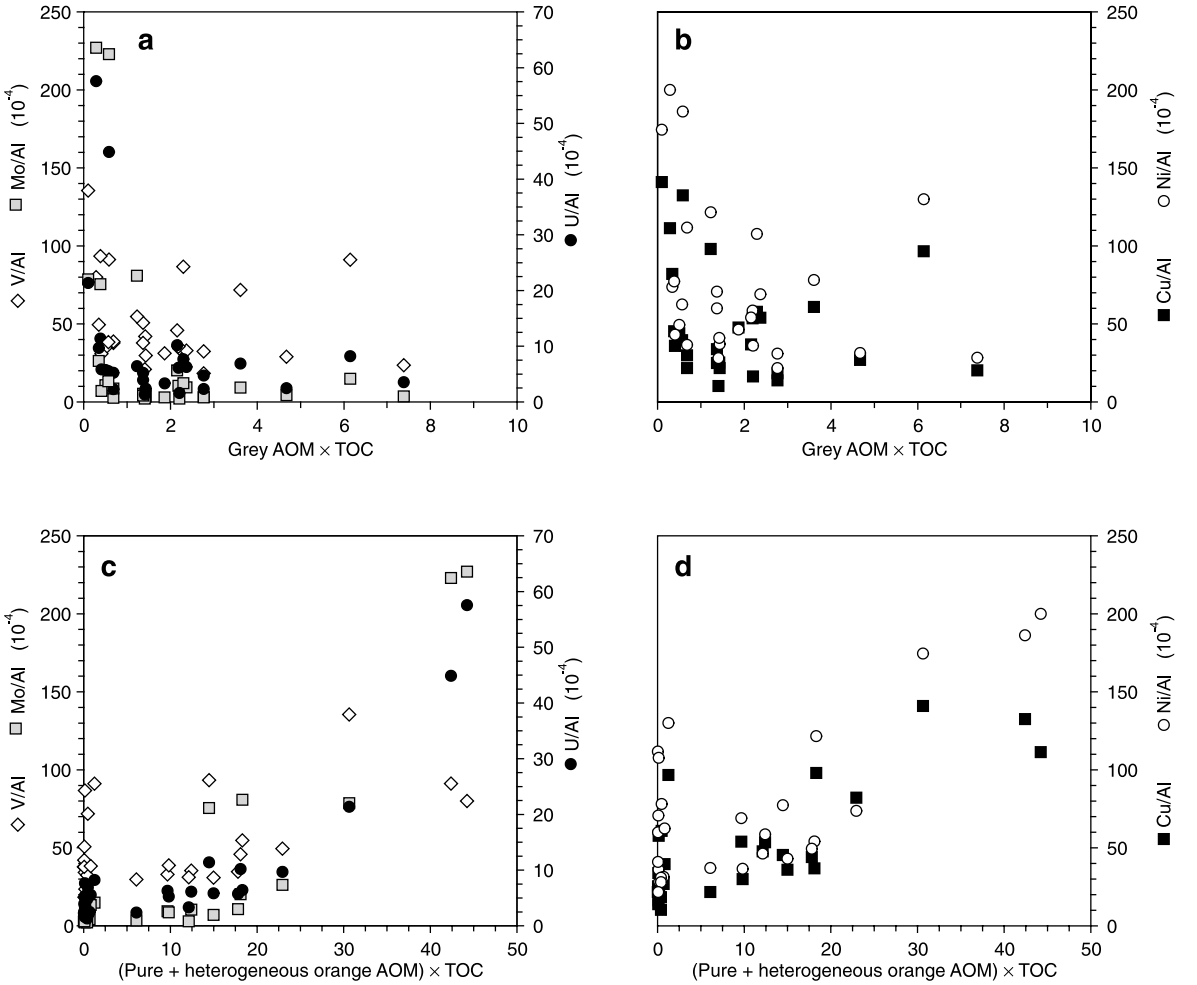

Fig. 16. Proportion of grey and pure+heterogeneous orange AOM in the sediment versus redox-sensitive (V, Mo and U) and sulphide-forming elements (Ni and Cu) contents normalised to Al for the organic-rich formation from Gorodische outcrop.

indicates the role of primary productivity and dysoxia–anoxia on the formation of sulphurised OM.

The depositional process of heterogeneous orange AOM-dominated samples appears quite similar to that of grey AOM, except that higher productivity and more severe dysoxia will allow abundant presence of reactive OM in the upper sediment and high rates of anoxic degradation leading to sulphurisation of reactive OM (Fig. 17b). Partial reoxidation of the sediment, attested by the presence of diverse and abundant benthos but probably of lower intensity than during marls deposition, allowed bioturbation and partial degradation of the remaining reactive OM present in the sediment (Fig. 17b).

6. Palaeoenvironmental interpretation

6.1. Palaeooxygenation

The results for the organic-rich unit from the Gorodische outcrop reflect the complex relationships that link primary productivity, redox conditions of bottom waters and upper sediment, and

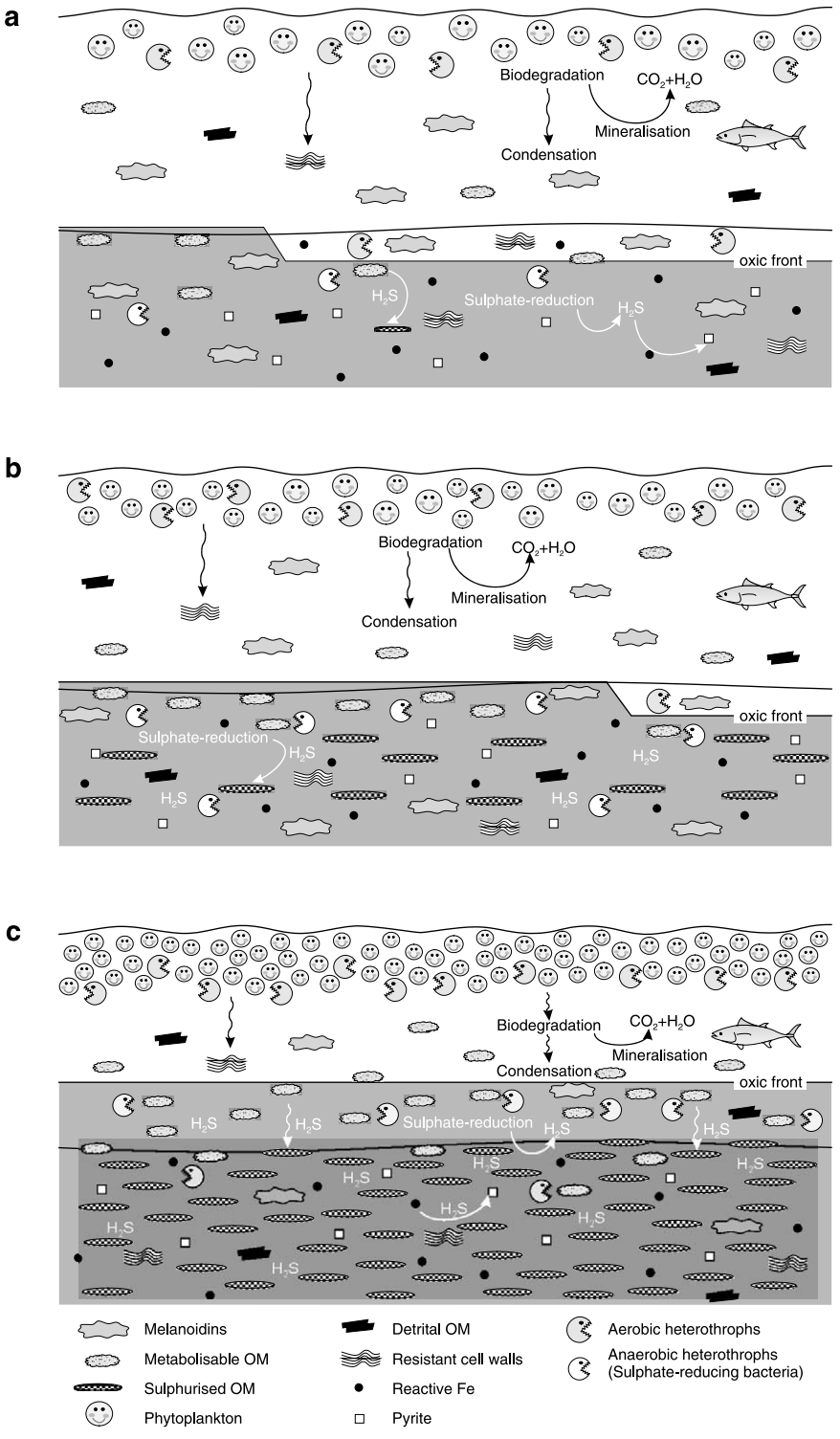
a
Biodegradation
CO_2+H_2O
Mineralisation
Condensation
oxic front
H_2S
Sulphate-reduction
H_2S
b
Biodegradation
CO_2+H_2O
Mineralisation
Condensation
oxic front
Sulphate-reduction
H_2S
H_2S
H_2S
H_2S
c
Biodegradation
CO_2+H_2O
Mineralisation
Condensation
oxic front
H_2S
H_2S
Sulphate-reduction
H_2S
H_2S
H_2S
H_2S
H_2S
H_2S
H_2S
H_2S
Melanoidins
Metabolisable OM
Sulphurised OM
Phytoplankton
Detrital OM
Resistant cell walls
Reactive Fe
Pyrite
Aerobic heterothrophs
Anaerobic heterothrophs
(Sulphate-reducing bacteria)

OM preservation processes. From the above discussion, it appears that TOC and HI variations in Go 11 level more or less directly reflect the mean palaeooxygenation of the bottom waters and upper sediment, which, in turn, is directly influenced by the primary productivity. A curve of mean palaeooxygenation of the upper sediment can therefore be constructed, on the basis of TOC and HI values and dominant AOM. Mean oxygenation levels from 1 to 6 were defined with level 1 corresponding to a good oxygenation (TOC $<$ 2%, grey AOM); level 2, relatively good oxygenation (2 $\leq$ TOC $<$ 5%, grey AOM); level 3, moderate oxygenation (5 $\leq$ TOC, grey AOM); level 4 low oxygenation (TOC $<$ 20%, heterogeneous orange AOM); level 5, very low oxygenation (20 $\leq$ TOC $<$ 40%, heterogeneous orange AOM); level 6, anoxia (TOC $\geq$ 40%, pure orange AOM). This pattern was applied to level 11 of the Gorodische section and extended to the underlying levels of Early and Middle Volgian age, considering that the same processes accounted for OM features (Fig. 18).

The general trend (in grey) indicates good oxygenation during the Early Volgian (Go 5–8) with an episode of slightly lower oxygenation at the end of the Early Volgian (Fig. 18). A return to good oxygenation is observed at the beginning of the Middle Volgian (Go 9 and Go 10 levels). Go 11 level is characterised by a sharp change to lower oxygenation, with a lower part predominantly moderately oxygenated and a higher part predominantly very low oxygenated. The black curve, directly reflects the black shale and marl alternations of Go 11 level. Despite the lack of supporting data other than the short deposition of the organic rich formation – less than one ammonite subzone, a few hundred thousand years – and by analogy with the metric alternations of many Mesozoic OM-rich formations, these marl–black shale alternations may be accounted for by climatic oscillations.

6.2. Origin and significance of clay minerals

Clay assemblages dominantly composed of illite, smectites and kaolinite are common in Upper Jurassic sediments (Chamley, 1989). The relative proportions of these minerals result from various parameters such as climate, sea level changes or detrital sources. By contrast, to the best of our knowledge, the occurrence of palygorskite has never been mentioned in other Late Jurassic deposits. This mineral, also observed by Ruffell et al. (2002), is restricted to the Gorodische section.

The occurrence of smectite and illite–smectite mixed layers is indicative of weak influence of burial diagenesis (Chamley, 1989), which is consistent with the low T_{max} values. Clay mineral assemblage is therefore dominantly detrital in origin. The variations in relative proportions of these minerals may therefore be interpreted in terms of palaeoenvironment. The evolution of clay mineralogy in the Gorodische section was interpreted by Chimkyavichus (1986) as reflecting the changing distance from the shoreline due to tectono-eustatic variations, while Ruffell et al. (2002) mostly interpreted the decrease in kaolinite as reflecting an episode of increased aridity which is well documented in Europe (Hallam et al., 1991). Due to their different settling modes (Gibbs, 1977) the opposite evolution of the kaolinite–illite and smectite contents is often considered as an indicator of the distance to the shoreline, or of the sea level fluctuations. The sharp increase in smectite and decrease in kaolinite content in Go 11 level could be consistent with a sea level rise as different eustatic charts show a high sea level during the *D. panderi* ammonite Zone (Haq et al., 1988; Sahagian et al., 1996; Hardenbol et al., 1998). However, a sharp sea level fall documented by Sahagian et al. (1996) at the end of the Early Volgian in the neighbouring Moscow Basin is not particularly marked in the clay mineralogy of the Gorodische section. It is therefore

Fig. 17. Reconstruction of the depositional palaeoenvironment for the different classes of samples in the organic-rich unit from the Gorodische outcrop. (a) Deposition of the grey AOM-dominated samples (most of the marls). (b) Deposition of the heterogeneous orange AOM-dominated samples (most of the black shales). (c) Deposition of the pure orange AOM-dominated samples (level *f*).

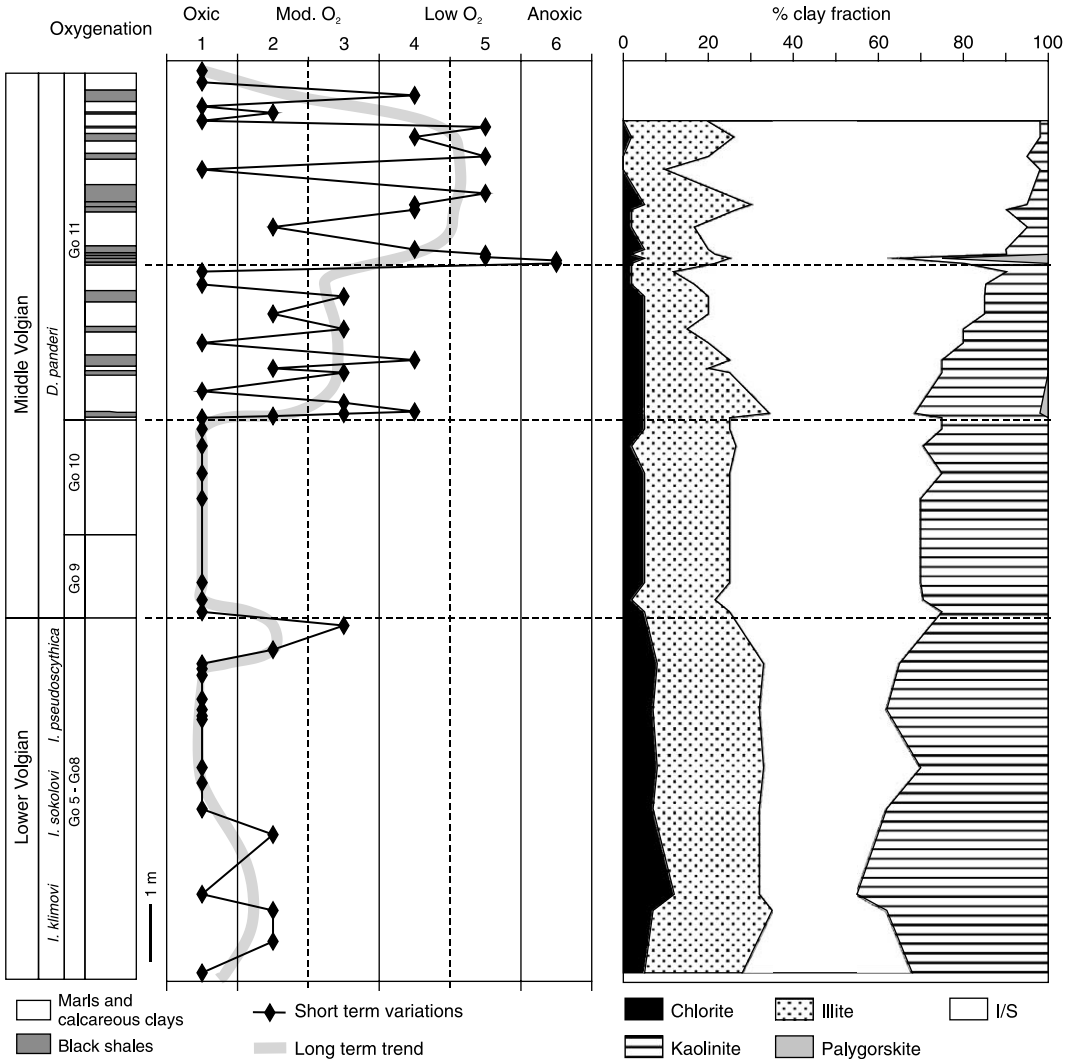

Fig. 18. Evolution of the reconstructed mean palaeooxygenation level compared to the clay minerals variation for the Volgian deposits of Gorodische outcrop.

likely that due to its location in the central part of the middle Volga Basin and long distance to the detrital sources (Thierry et al., 2000), the sea level variations only weakly affected clay composition in the Gorodische setting. The major trend in the clay mineralogy (decreasing kaolinite and increasing smectites) is, therefore, preferentially attributed to a climatic change from humid to arid conditions (Ruffell et al., 2002). The emergence of the southern part of the Russian Platform during the Volgian (Markovskii, 1959; Beznosov et al., 1978) may have also favoured the change in clay mineralogy by leading to the formation of smectite-containing soils or erosion of smectite-containing sediments. The occurrence of palygorskite which typifies evaporitic environments is, however, consistent with aridification.

6.3. Depositional model

The long-term evolution of the oxygenation curve is parallel with the evolution of the clay

mineralogy (Fig. 18). Indeed, in Go 5–8, Go 9 and Go 10 levels, where the clay mineralogy only shows a very slight evolution, the oxygenation remains fairly good. The sharp change to lower oxygenation in Go 11 level coincides with the beginning of the rapid decrease of kaolinite and increase of smectites. The second part of Go 11 level, marked by even lower oxygenation, corresponds to the part where the lowest kaolinite content and highest smectite content are observed.

On a first order, the deposition of the organic-rich Go 11 level appears to be closely linked to the major climatic aridification recorded in the clay mineralogy (Fig. 18). The common depositional model which links arid climate and OM deposition is based on the development of bottom water anoxia due to the formation of warm saline deep waters (e.g. Pratt and King, 1986, for the Aptian–Albian deposits from Italian Appenine, or Miller, 1990, for the Kimmeridge Clay Formation). The formation of dense saline bottom waters on the Russian Platform is consistent with the presence of evaporites in its southern part (Markovskii, 1959; Beznosov et al., 1978), and with an increase of water salinity during the Uppermost Jurassic, indicated by the Sr and Mg contents of belemnite rostra (Riboulleau et al., 1998). However, numerous data in this study, as well as in Ruffell et al. (2002), indicate that primary productivity was also increased. The relationship between aridification and primary productivity is more difficult to assess. The general concept is that nutrient inputs to a basin, leading to a high phytoplanktonic productivity, are linked to high rainfall and continental runoff, and are therefore related to a humid climate in the absence of upwelling (e.g. Rossignol-Strick, 1983; Ramdani, 1996; Röhl et al., 2001). The pattern observed in the Gorodische section contrasts with this general conception, since it appears that the aridification and primary productivity increase are closely linked. Ruffell et al. (2002) also came to the same conclusion, considering likely that nutrient inputs were not related to runoff.

In the Quaternary, it is well known that phytoplancton productivity may be enhanced in relation to aridity (Falkowski et al., 1998). This phenomenon is related to increased transport of atmospheric dust during arid periods and therefore increased aeolian input of reactive iron – Fe-oxihydroxides coating clay minerals – to the basins (Martin, 1990; Falkowski et al., 1998). Iron is indeed involved in phytoplankton metabolism and is proved to be a limiting factor toward phytoplankton productivity (Falkowski et al., 1998; Chester, 2000). An iron-stimulated productivity was, in particular, proposed to explain the increased phytoplankton productivity observed during the last glacial maximum, when climate was more arid and atmospheric dust was more abundant (Martin, 1990). Similarly, this mechanism could account for the increased primary productivity during an arid period in the Kashpir Oil Shales. The presence of the aridity proxy palygorskite, which is often wind transported (Chamley, 1989), in the very first occurring black shales as well as in the TOC-richest levels, supports such an hypothesis.

The depositional model we propose for the Kashpir oil shales formation is summarised in Fig. 19. As previously discussed, the arid climate was favourable to the formation of evaporite-prone sabkha-type environments in the southern part of the Russian Platform, and formation of dense saline bottom water. Salinity stratification could therefore develop, probably strengthened by the existence of a thermocline. Under these conditions, nutrients were trapped under the pycnocline. Primary productivity was moderate to low, leading to low fluxes of OM to the sediment and, therefore, to only low consumption of oxygen under the pycnocline, as attested by the diversified benthic fauna and presence of bioturbation/burrowing (Fig. 19, ①).

Storms are predicted on the Russian Platform during winter by recent modelling of Late Jurassic climate (Rees et al., 2000). Consistent with this, erosional surfaces are described in Go 11 level by some authors (Vishnevskaya et al., 1999; Baraboshkin, personal communication). Episodes of OM deposition, in relation to increased primary productivity, are proposed to have occurred during periods of increased storm activity. Disruption of the water column stratification by storm waves released the nutrients trapped under the pycnocline to the surface waters. Increased wind activity

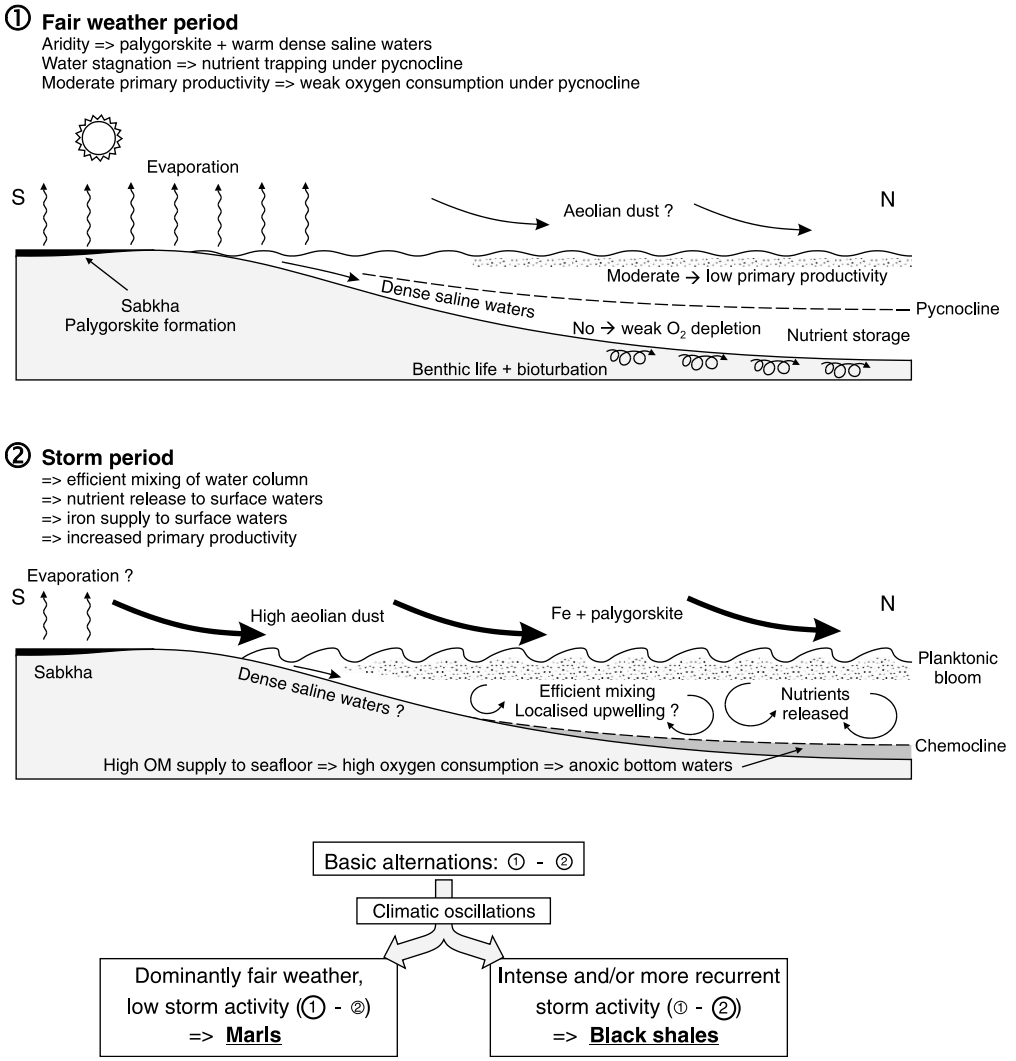

Fig. 19. Depositional model for the Kashpir Oil Shales Formation. During generally increasing arid conditions, fair weather periods are favourable to water stratification, low primary productivity and normal oxygenation of the upper sediment (①). OM deposition mostly occurs during storm periods, when phytoplankton blooms are promoted by nutrient release to the surface waters and aeolian supply of iron (②). Marl levels correspond to epochs of generally poorly developed storm periods, leading to moderately low OM deposition and efficient OM mineralisation during fair weather-dominated periods (① > ②). Black shales levels correspond to epochs of generally stronger storm activity leading to high OM deposition and less efficient reoxygenation of the sea floor during fair weather periods (① < ②).

also led to enhanced aeolian transport of iron-coated particles, and palygorskite, to the basin. The combination of nutrients and Fe supply to the surface waters promoted phytoplankton blooms. High fluxes of OM reached the sediment, leading to high oxygen consumption and anoxia development in the sediment and, possibly, above the sediment–water interface (Fig. 19, ②). On the basis of wind circulation patterns proposed by the qualitative or atmospheric global circulation model, coastal upwelling could have also occurred locally during these periods (Parrish and Curtis, 1982; Moore et al., 1992); but, due to its restricted location this latter phenomenon cannot

by itself account for the widespread occurrence of OM-rich deposits on the Russian Platform.

As previously discussed, the recurrent alternation of sea floor anoxia and oxygenation, rather than long-term bottom water anoxia, is attested in both marls and black shales, by the geochemical and ecological data. It is also consistent with the $\delta^{13}C$ trends of the OM and of belemnite rostra (Riboulleau et al., 1998; Riboulleau, 2000). This process – ①−② basic alternations of Fig. 19 – gave to the formation its very peculiar combination of anoxic and oxic characteristics. The marl and black shale alternations are inferred to have formed in relation to climate oscillations: marls corresponding to epochs of generally poorly developed storm periods, leading to moderately low OM deposition and efficient mineralisation during fair weather-dominated periods (① > ②, Fig. 19), and black shales forming during epochs of generally stronger storm activity leading to high OM deposition and less efficient reoxygenation of the sea floor during fair weather periods (① < ②, Fig. 19).

7. Conclusion

The multidisciplinary study of the Volgian deposits of the Gorodische section allowed us to determine the conditions that led to the deposition of the organic-rich Kashpir Oil Shales Formation. The variations in OM quality and quantity in the Kashpir Oil Shales are related to the different contribution of two contrasting classes of organic particles. One class is aliphatic, enriched in sulphur and formed by natural sulphurisation in anoxic sediment while the other is poorly aliphatic and formed by random polymerisation of biodegradation products in oxygenated sediment. These different classes of organic particles reflect different early diagenetic and palaeoenvironmental conditions.

The clay mineral content indicates that deposition of the organic-rich formation occurred during a period of increasing aridity. This climate change was favourable to the stratification of the water column through the formation of relatively oxic dense saline water in the southern part of the Russian Platform, and to increased transport of atmospheric dust. OM deposition mainly occurred during storm periods, when phytoplankton activity was fostered by nutrient release to the surface waters and aeolian supply of iron. Short-term alternations of storm and fair weather periods are attested by the geochemical and ecological data. They may correspond to seasonal or pluriannual variations. The marl and black shale alternations are probably related to climatic oscillations, marls being deposited during periods of dominant fair weather, and black shales during periods of more developed storm activity.

Acknowledgements

This research was sponsored by Peri–Tethys project 95-96/28 and Société de Secours des Amis des Sciences (A.R.). We wish to thank P. Recourt and D. Malengros (Lille) for the X ray and LECO analyses, F. Savignac (UPMC) and D. Keravis (Orléans) for Rock Eval analyses and R. Caron (UPMC) for the thin sections. E. Lallier-Vergès, F. Surlyk, P. Wignall and an anonymous reviewer are acknowledged for constructive comments on earlier versions of the manuscript.

References

Aller, R.C., Mackin, J.E., Cox, R.T.J., 1986. Diagenesis of Fe and S in Amazon inner shelf muds: apparent dominance of Fe reduction and implications for the genesis of ironstones. Deep Sea Res. 6, 263–289.

Arthur, M.A., Jenkyns, H.C., Brumsack, H.J., Schlanger, S.O., 1990. Stratigraphy, geochemistry, and paleoceanography of organic carbon-rich Cretaceous sequences: Background and plans for research. In: Ginsburg, R.N., Beaudoin, B. (Eds.), Cretaceous Resources, Events and Rhythms. Kluwer Academic Publishers, Boston, MA, pp. 75–119.

Baudin, F., 1995. Depositional controls on Mesozoic source rocks in the Tethys. In: Huc, A.Y. (Ed.), Paleogeography, Paleoclimate, and Source Rocks. Am. Assoc. Pet. Geol. Stud. Geol. 40, Tulsa, pp. 191–211.

Bein, A., Almogi-Labin, A., Sass, E., 1990. Sulfur sinks and organic carbon relationships in Cretaceous organic-rich carbonates: implications for evaluation of oxygen poor depositional environments. Am. J. Sci. 290, 882–911.

Berner, R.A., Raiswell, R., 1983. Burial of organic carbon and

pyrite sulfur in sediments over Phanerozoic time: a new theory. Geochim. Cosmochim. Acta 47, 855–862.

Berner, R.A., Raiswell, R., 1984. C/S methods for distinguishing freshwater from marine sedimentary rocks. Geology 12, 365–368.

Berner, R.A., Westrich, J.T., 1985. Bioturbation and the early diagenesis of carbon and sulfur. Am. J. Sci. 285, 193–206.

Bertrand, P., Lallier-Vergès, E., Martinez, L., Pradier, B., Tremblay, P., Huc, A.Y., Jouhannel, R., Tricard, J.-P., 1990. Examples of spatial relationship between organic matter and mineral groundmass in the microstructure of the organic-rich Dorset Formation rocks, Great Britain. In: Durand, B., Béhar, F. (Eds.), Advances in Organic Geochemistry 1989. Org. Geochem. 16, 661–675.

Beznosov, N.V., Gorbatchik, T.N., Michailova, I.A., Pergament, M.A., 1978. Soviet Union. In: Moullade, M., Nairn, A.E.M. (Eds.), The Phanerozoïc Geology of the World, II, The Mesozoïc. Elsevier, Amsterdam, pp. 5–53.

Bialkowski, A., Tribovillard, N.-P., Vergès, E., Deconinck, J.-F., 2000. Etude haute résolution de la distribution et de la granulométrie des constituants organiques sédimentaires dans le Kimméridgien-Tithonien du Boulonnais (Nord de la France). Application à l'analyse séquentielle. C. R. Acad. Sci. (Paris) 331, 451–458.

Boussafir, M., 1994. Microtexture et structure ultrafine des roches et matières organiques pétroligènes: Nature et mode de fossilisation de la matière organique dans les séries organosédimentaires cycliques du Kimméridgien d'Angleterre. PhD Thesis, Université d'Orléans, France, 188 pp.

Boussafir, M., Gelin, F., Lallier-Vergès, E., Derenne, S., Bertrand, P., Largeau, C., 1995. Electron microscopy and pyrolysis of kerogen from the Kimmeridge Clay Formation, UK: Source organisms, preservation processes, and origin of the microcycles. Geochim. Cosmochim. Acta 59, 3731–3747.

Brown, G., Brindley, G.W., 1980. X-ray diffraction procedures for clay mineral identification. In: Brindley, G.W., Brown, G. (Eds.), Crystal Structures of Clay Minerals and Their X-ray Identification. London, Mineral. Soc. Monogr. 5, pp. 305–359.

Brumsack, H.J., 1986. The inorganic geochemistry of Cretaceous black shales (DSDP leg 41) in comparison to modern upwelling sediments from the Gulf of California. In: Summerhayes, C.P., Shackleton, N.J. (Eds.), North Atlantic Palaeoceanography. Geol. Soc. London Spec. Publ. 21, 447–462.

Brumsack, H.J., 1989. Geochemistry of recent TOC-rich sediments from the Gulf of California and the Black Sea. Geol. Rundsch. 78, 851–882.

Calvert, S.E., Perdersen, T.F., 1993. Geochemistry of Recent oxic and anoxic sediment: implication for the geological record. Mar. Geol. 113, 67–88.

Caron, M., Robaszynski, F., Amedro, F., Baudin, F., Deconinck, J.-F., Hochuli, P., von Salis-Perch Nielsen, K., Tribovillard, N., 1999. Estimation de la durée de l'évènement anoxique global au passage Cénomanien/Turonien. Approche cyclostratigraphique dans la formation de Bahloul en Tunisie centrale. Bull. Soc. Géol. France 170, 145–169.

Chamley, H., 1989. Clay Sedimentology. Springer, Berlin, 624 pp.

Chester, R., 2000. Marine Geochemistry, 2nd edn. Blackwell, London, 520 pp.

Chimkyavichus, P.I., 1986. Lithology and clay minerals of Upper Jurassic deposits of the central part of East European Platform (in Russian). In: Mesezhnikov, M.S. (Ed.), Jurassic Deposits of the Russian Platform. Leningrad Oil and Gas Institute, Leningrad, pp. 180–192.

Derenne, S., Largeau, C., Casadevall, E., Berkaloff, C., Rousseau, B., 1991. Chemical evidence of kerogen formation in source rocks and oil shales via selective preservation of thin resistant outer walls of microalgae: Origin of ultralaminae. Geochim. Cosmochim. Acta 55, 1041–1050.

Durand, B., Nicaise, G., 1980. Procedures for kerogen isolation. In: Durand, B. (Ed.), Kerogen. Technip, Paris, pp. 33–53.

Espitalié, J., Deroo, G., Marquis F., 1985–1986. La pyrolyse Rock Eval et ses applications. Rev. Inst. Fr. Pét. 40, 563–578; 40, 755–784; 41, 73–89.

Falkowski, P.G., Barber, R.T., Smetacek, V., 1998. Biogeochemical controls and feedbacks on ocean primary production. Science 281, 200–206.

Gerasimov, P.A., Mikhailov, N.P., 1966. Volgian stage and the geostratigraphical scale for the Upper series of the Jurassic system (in Russian). Izv. Akad. Nauk SSSR Ser. Geol. 2, 118–138.

Gibbs, R.J., 1977. Clay mineral segregation in the marine environment. J. Sediment. Petrol. 47, 237–243.

Hallam, A., 1987. Mesozoic marine organic-rich shales. In: Brooks, J., Fleet, A.J. (Eds.), Marine Petroleum Source Rocks. Geol. Soc. London Spec. Publ. 26, 251–261.

Hallam, A., Grose, J.A., Ruffell, A.H., 1991. Palaeoclimatic significance of changes in clay mineralogy across the Jurassic–Cretaceous boundary in England and France. Palaeogeogr. Palaeoclimatol. Palaeoecol. 81, 173–187.

Hantzpergue, P., Baudin, F., Mitta, V., Olferiev, A., Zakharov, V., 1998. The Upper Jurassic of the Volga basin: ammonite biostratigraphy and occurence of organic carbon-rich facies. Correlations between boreal-subboreal and submediterranean provinces. In: Crasquin-Soleau, S., Barrier, E. (Eds.), Peri-Tethys Memoir 4: Epicratonic Basins of Peri-Tethyan Platforms. Mém. Mus. Natl. Hist. Nat. 179, 9–33.

Haq, B.U., Hardenbol, J., Vail, P.R., 1988. Mesozoic and Cenozoic chronostratigraphy and cycles of sea-level change. In: Wilgus, C.K., Hastings, B.S., Kendali, C.G.St.C., Posamentier, H.W., Ross, C.A., Van Wagoner, J.C. (Eds.), Sea-Level Changes: An Integrated Approach. SEPM Spec. Publ. 42, 71–108.

Hardenbol, J., Thierry, J., Farley, M.B., Jacquin, T., De Graciansky, P.-C., Vail, P.R., 1998. Jurassic sequence chronostratigraphy. In: De Graciansky, P.-C., Hardenbol, J., Jacquin, T., Vail, P.R. (Eds.), Mesozoic and Cenozoic Sequence

Stratigraphy of European Basins. Spec. Publ. Soc. Sediment. Geol. 60, 786 pp.

Holtzapffel, T., 1985. Les minéraux argileux: Préparation, analyse diffractométrique et détermination. Société Géologique du Nord Publications, Villeneuve d'Ascq, 136 pp.

Huc, A.Y., Lallier-Vergès, E., Bertrand, P., Carpentier, B., Hollander, D.J., 1992. Organic matter response to change of depositional environment in Kimmeridgian shales, Dorset, U.K. In: Whelan, J.K., Farrington, J.W. (Eds.), Organic Matter: Productivity and Preservation in Recent and Ancient Sediments. Columbia University Press, New York, pp. 469–486.

Hulthe, G., Hulth, S., Hall, P.O.J., 1998. Effect of oxygen on degradation rate of refractory and labile organic matter in continental margin sediments. Geochim. Cosmochim. Acta 62, 1319–1328.

Joachimski, M.M., Ostertag-Henning, C., Pancost, R.D., Strauss, H., Freeman, K.H., Littke, R., Sinninghe Damsté, J.S., Racki, G., 2001. Water column anoxia, enhanced productivity and concomitant changes in $\delta^{13}C$ and $\delta^{34}S$ across the Frasnian–Famennian boundary (Kowala – Holy Cross Mountains/Poland). Chem. Geol. 175, 109–131.

Lafargue, E., Marquis, F., Pillot, D., 1998. Rock Eval 6 applications in hydrocarbon exploration, production and soil contamination studies. Rev. Ist. Fr. Pét. 53, 421–437.

Lallier-Vergès, E., Bertrand, P., Desprairies, A., 1993a. Organic matter composition and sulfate reduction intensity in Oman Margin sediments. Mar. Geol. 112, 57–69.

Lallier-Vergès, E., Bertrand, P., Huc, A.Y., Bückel, D., Tremblay, P., 1993b. Control of the preservation of organic matter by productivity and sulphate reduction in Kimmeridgian shales from Dorset (UK). Mar. Pet. Geol. 10, 600–605.

Lallier-Vergès, E., Tribovillard, N.P., Bertrand, P., 1995. Organic matter accumulation. The organic cyclicities of the Kimmeridge Clay Formation (Yorkshire, GB) and the Recent Maar sediments (Lac du Bouchet, France). Lect. Notes Earth Sci. 57, 188 pp.

Largeau, C., Derenne, S., Casadevall, E., Berkaloff, C., Corolleur, M., Lugardon, B., Raynaud, J.-F., Connan, J., 1990. Occurrence and origin of 'ultralaminar' structures in 'amorphous' kerogens of various source rocks and oil shales. In: Durand, B., Behar, F. (Eds.), Advances in Organic Geochemistry 1989. Org. Geochem. 16, 889–895.

Leith, T.L., Weiss, H.M., Mørk, A., Århus, N., Elvebakk, G., Embry, A.F., Brooks, P.W., Stewart, K.R., Pchelina, T.M., Bro, E.G., Verba, M.L., Danyushevskaya, A., Borisov, A.V., 1992. Mesozoic hydrocarbon source-rocks of the Arctic region. In: Vorren, T.O., Bergsager, E., Dahl-Stamnes, Ø.A., Holter, E., Johansen, B., Lie, E., Lund, T.B. (Eds.), Arctic Geology and Petroleum Potential Vol. 2. Elsevier, Amsterdam, pp. 1–25.

Leventhal, J.S., 1983. An interpretation of carbon and sulfur relationships in Black Sea sediments as indicators of environments of deposition. Geochim. Cosmochim. Acta 47, 133–137.

Littke, R., Klussmann, U., Kroos, B., Leythaeuser, D., 1991. Quantification of loss of calcite, pyrite, and organic matter due to weathering of Toarcian black shales and effects on kerogen and bitumen characteristics. Geochim. Cosmochim. Acta 55, 3369–3378.

Lord, A.R., Cooper, M.K.E., Corbett, P.W.M., Fuller, N.G., Rawson, P.F., Rees, A.J.J., 1987. Microbiostratigraphy of the Volgian stage (Upper Jurassic), Volga river, USSR. N. Jahrb. Geol. Paläont. Mh. 10, 577–605.

Markovskii, A.P., 1959. Structure Géologique de l'URSS, tome 1 Stratigraphie, fascicule 4. CNRS, Paris, 652 pp.

Martin, J.H., 1990. Glacial–interglacial CO_2 change: the iron hypothesis. Paleoceanography 5, 1–13.

Mesezhnikov, M.S., Dain, L.G., Kuznetsova, K.I., Yakovleva, S.P., 1977. Jurassic/Cretaceous boundary beds in the middle Volga area (A prospectus to geological excursions). In: International Colloguy on the Upper Jurassic Stratigraphy and Jurassic/Cretaceous Boundary in the Boreal Realm. Ministry of Geology of the USSR, VNIGRI, Leningrad, pp. 21–34.

Miller, R.G., 1990. A paleoceanographic approach to the Kimmeridge Clay Formation. In: Huc, A.Y. (Ed.), Deposition of Organic Facies. Am. Assoc. Pet. Geol. Stud. Geol. 30, 13–26.

Mongenot, T., Derenne, S., Largeau, C., Tribovillard, N.-P., Lalier-Vergès, E., Dessort, D., Connan, J., 1999. Spectroscopic, kinetic and pyrolytic studies of the sulphur-rich Orbagnoux deposit (Upper Kimmeridgian, Jura). Org. Geochem. 30, 39–56.

Mongenot, T., Riboulleau, A., Garcette-Lepecq, A., Derenne, S., Pouet, Y., Baudin, F., Largeau, C., 2001. Occurrence of proteinaceous moieties in S- and O-rich Late Tithonian kerogen (Kashpir oil Shales, Russia). Org. Geochem. 32, 199–203.

Moore, G.T., Hayashida, D.N., Ross, C.A., Jacobson, S.R., 1992. Paleoclimate of the Kimmeridgian/Tithonian (Late Jurassic) world: I. Results using a general circulation model. Palaeogeogr. Palaeoclimatol. Palaeoecol. 93, 113–150.

Moore, D.M., Reynolds, R.C., 1989. X-Ray Diffraction and the Identification and Analysis of Clay Minerals. Oxford University Press, Oxford, 331 pp.

Orr, W.L., 1986. Kerogen/asphaltene/sulfur relationships in sulfur-rich Monterey oils. Org. Geochem. 10, 499–516.

Parrish, J.T., Curtis, R.L., 1982. Atmospheric circulation, upwelling, and organic-rich rocks in the Mesozoic and Cenozoic eras. Palaeogeogr. Palaeoclimatol. Palaeoecol. 40, 31–66.

Passier, H.F., Middelburg, J.J., van Os, B.J.H., de Lange, G.J., 1996. Diagenetic pyritisation under eastern Mediterranean sapropels caused by downward sulphide diffusion. Geochim. Cosmochim. Acta 60, 751–763.

Peulvé, S., de Leeuw, J.W., Sicre, M.-A., Baas, M., Saliot, A., 1996. Characterization of macromolecular organic matter in sediment traps from the northwestern Mediterranean Sea. Geochim. Cosmochim. Acta 60, 1239–1259.

Poirier, N., Derenne, S., Rouzaud, J.-N., Largeau, C., Mariotti, A., Balesdent, G., Maquet, J., 2000. Chemical structure and sources of the macromolecular, resistant, organic fraction isolated from a forest soil (Lacadée, South-west France). Org. Geochem. 31, 813–827.

Pradier, B., Bertrand, P., 1992. Etude à haute résolution d'un cycle du carbone organique de roche-mère du Kimméridgien du Yorkshire: Relation entre composition pétrographique du contenu organique observé in situ, teneur en carbone organique et qualité pétroligène. C. R. Acad. Sci. (Paris) 315, 187–192.

Pratt, L.M., 1984. Influence of paleoenvironmental factors on preservation of organic matter in middle Cretaceous Greenhorn Formation, Pueblo, Colorado. Am. Assoc. Pet. Geol. Bull. 68, 1146–1159.

Pratt, L.M., King, J.D., 1986. Variable marine productivity and high eolian input recorded by rythmic black shales in mid-Cretaceous pelagic deposits from central Italy. Paleoceanography 1, 507–522.

Raiswell, R., Berner, R.A., 1986. Pyrite and organic matter in Phanerozoic normal marine shales. Geochim. Cosmochim. Acta 50, 1967–1976.

Ramanampisoa, L., Bertrand, P., Disnar, J.-R., Lallier-Vergès, E., Pradier, B., Tribovillard, N.-P., 1992. Etude à haute résolution d'un cycle de carbone organique des argiles du Kimméridgien du Yorkshire (Grande Bretagne): résultats préliminaires de géochimie et de pétrographie organique. C. R. Acad. Sci. (Paris) 314, 1493–1498.

Ramdani, A., 1996. Les paramètres qui contrôlent la sédimentation cyclique de la 'Kimmeridge Clay Formation', dans le Bassin de Cleveland (Yorkshire, Grande-Bretagne). Comparaison avec le Boulonnais (France). PhD. Thesis, Université d'Orsay, Paris XI, 260 pp.

Raynaud, J.F., Lugardon, B., Lacrampe-Couloume, G., 1989. Structures lamellaires et bactéries, composants essentiels dela matière organique amorphe des roches mères. Bull. Cent. Rech. Explor. Prod. Elf-Aquitaine 13, 1–21.

Rees, P.M., Ziegler, A.M., Valdes, P.J., 2000. Jurassic phytogeography and climate: new data and model comparisons. In: Huber, B.T., MacLeod, K.G., Wing, S.L. (Eds.), Warm Climates in Earth History. Cambridge University Press, Cambridge, pp. 297–318.

Reynolds, R.C., 1980. Interstratified clay minerals. In: Brindley, G.W., Brown, G. (Eds.), Crystal Structures of Clay Minerals and Their X-ray Identification. London, Mineral. Soc. Monogr. 5, 249–303.

Riboulleau, A., 2000. Géochimie des black shales du Jurassique supérieur de la plate-forme russe. Processus de sédimentation et de préservation de la matière organique. PhD Thesis, Université Pierre et Marie Curie, Paris VI, 262 pp.

Riboulleau, A., Baudin, F., Daux, V., Hantzpergue, P., Renard, M., Zakharov, V., 1998. Evolution de la paléotempérature des eaux de la plate-forme russe au cours du Jurassique Supérieur. C. R. Acad. Sci. (Paris) 326, 239–246.

Riboulleau, A., Derenne, S., Largeau, C., Baudin, F., 2001. Origin of contrasted features and preservation pathways in kerogens from the Kashpir oil shales (Upper Jurassic, Russian Platform). Org. Geochem. 32, 647–665.

Riboulleau, A., Derenne, S., Sarret, G., Largeau, C., Baudin, F., Connan, J., 2000. Pyrolytic and spectroscopic study of sulphur-rich kerogen from the 'Kashpir oil shales' (Upper Jurassic; Russian Platform). In: Yalçin, M.N., Inan, S. (Eds), Advances in Organic Geochemistry 1999. Pergamon, Oxford. Org. Geochem. 31, 1641–1661.

Röhl, H.-J., Schmidt-Röhl, A., Oschmann, W., Frimmel, A., Schwark, L., 2001. The Posidonia Shale (Lower Toarcian) of SW-Germany: an oxygen depleted ecosystem controlled by sea level and paleoclimate. Palaeogeogr. Palaeoclimatol. Palaeoecol. 165, 27–52.

Rossignol-Strick, M., 1983. African monsoon, an immediate response to orbital insolation. Nature 303, 46–49.

Russell, P.L., 1990. Oil Shales of the World, Their Origin, Occurence and Exploitation. Pergamon Press, Oxford, 753 pp.

Ruffell, A.H., Price, G.D., Mutterlose, J., Kessels, K., Baraboshkin, E., Gröcke, D.R., 2002. Late Jurassic climate change in the Volga Basin (SE Russia): clay mineral and calcareous nannofossil evidence. Geol. J. 37, 17–33.

Sahagian, D., Pinous, O., Olferiev, A., Zakharov, V., 1996. Eustatic curve for the Middle Jurassic-Cretaceous based on Russian Platform and Siberian sratigraphy: zonal resolution. Am. Assoc. Pet. Geol. Bull. 80, 1433–1458.

Sinninghe Damsté, J.S., de Leeuw, J.W., 1989. Analysis, structure and geochemical significance of organically-bound sulphur in the geosphere: state of the art and future research. Org. Geochem. 16, 1077–1101.

Suits, N.S., Arthur, M.A., 2000. Sulfur diagenesis and partitioning in Holocene Peru shelf and upper slope sediments. Chem. Geol. 163, 219–234.

Thierry, J. et al. (41 co-authors), 2000. Early Tithonian. In: Dercourt, J., Gaetani, M., Vrielynck, B., Barrier, E., Biju-Duval, B., Brunet, M.F., Cadet, J.P., Crasquin, S., Sandulescu, M. (Eds.), Atlas Peri-Tethys, Palaeogeographical Maps. CCGM/CGMW, Paris, map 11.

Tissot, B.P., Welte, D.H., 1978. Petroleum Formation and Occurrence. Springer, New York, 700 pp.

Tribovillard, N., Bialkowski, A., Tyson, R.V., Lallier-Vergès, E., Deconinck, J.-F., 2001. Organic facies variation in the late Kimmeridgian of the Boulonnais area (northernmost France). Mar. Pet. Geol. 18, 371–389.

Tribovillard, N.P., Desprairies, A., Lallier-Vergès, E., Bertrand, P., Moureau, N., Ramdani, A., Ramanampisoa, L., 1994. Geochemical study of organic-rich cycles from the Kimmeridge Clay Formation of Yorkshire (UK): productivity versus anoxia. Palaeogeogr. Palaeoclimatol. Palaeoecol. 108, 165–181.

Tyson, R.V., Pearson, T.H., 1991. Modern and ancient continental shelf anoxia: an overview. In: Tyson, R.V., Pearson, T.H. (Eds.), Modern and Ancient Continental Shelf Anoxia. Geol. Soc. London Spec. Publ. 58, 1–24.

Ulmishek, G.F., Klemme, H.D., 1990. Depositional Controls, Distribution, and Effectiveness of World Petroleum Source Rocks. U.S. Geol. Surv. Bull. 1931, 60 pp.

van Bergen, P.F., Bull, I.D., Poulton, P.R., Evershed, R.P., 1997. Organic geochemical studies of soils from the Rothamsted Classical Experiment – I. Total lipid extracts, solvent insoluble residues and humic acids from Broadbalk Wilderness. Org. Geochem. 26, 117–135.

van Heemst, J.D.H., Baas, M., de Leeuw, J.W., Renner, R.,

1993. Molecular characterization of marine dissolved organic matter (DOM). In: Øygard, O.K. (Ed.), Organic Geochemistry. Folch Hurtigtryhk, pp. 694–698.

Vishnevskaya, V.S., de Wever, P., Baraboshkin, E.Y., Bogdanov, N.A., Bragin, N.Y., Bragina, L.G., Kostyuchenko, A.S., Lambert, E., Malinovsky, Y.M., Sedaeva, K.M., Zukova, G.A., 1999. New stratigraphic and palaeogeographic data on Upper Jurassic to Cretaceous deposits from the eastern periphery of the Russian Platform (Russia). Geodiversitas 21, 347–363.

Wedepohl, K.H., 1971. Environmental influences on the chemical composition of shales and clays. In: Ahrens, L.H., Press, F., Runcorn, S.K., Urey, H.C. (Eds.), Physics and Chemistry of the Earth. Pergamon, Oxford, pp. 305–333.

Wedepohl, K.H., 1991. The composition of the upper Earth's crust and the natural cycles of selected metals. In: Merian, E. (Ed.), Metals and Their Compounds in the Environment. VCH-Verlagsgesellschaft, Weinheim, pp. 3–17.

Whitaker, M.F., 1984. The usage of palynology in definition of Troll Field geology. In: Reduction of Uncertainties in Innovative Reservoir Geomodelling. 6th Offshore Northern Seas Conference and Exhibition. Stavanger, 1984, paper G6.

Zegouagh, Y., Derenne, S., Largeau, C., Bertrand, P., Sicre, M.-A., Saliot, A., Rousseau, B., 1999. Refractory organic matter in sediments from the North-West African upwelling system: abundance, chemical structure and origin. Org. Geochem. 30, 101–118.